Ultrasonics Sonochemistry 27 (2015) 210–234

Contents lists available at ScienceDirect

Ultrasonics Sonochemistry

journal homepage: www.elsevier.com/locate/ultson

Review

A review on sonoelectrochemical technology as an upcoming alternative for pollutant degradation

Binota Thokchom [a], Aniruddha B. Pandit [b,*], Pengpeng Qiu [a], Beomguk Park [a], Jongbok Choi [a], Jeehyeong Khim [a,*]

[a] School of Civil, Environmental and Architectural Engineering, Korea University, 5-ga, Anam-dong, Seongbuk-gu, Seoul 136-701, South Korea
[b] Chemical Engineering Department, Institute of Chemical Technology, Matunga, Mumbai 40019, India

ARTICLE INFO

Article history:
Received 3 January 2015
Received in revised form 8 May 2015
Accepted 13 May 2015
Available online 16 May 2015

Keywords:
Sonoelectrochemical technology
Pollutant degradation
Synergy
Reactor configuration
System parameters

ABSTRACT

Sonoelectrochemical process has emerged as a novel integrated technology for various applications starting from sonoelectroplating till the remediation of a wide range of contaminants. Although a promising new technology, the application of sonoelectrochemical technology for pollutant degradation are mostly on a laboratory scale, utilizing the conventional reactor configuration of the electrolytic vessel and ultrasonic horns dipped in it. This type of configuration has been believed to be responsible for its sluggish evolution with lower reproducibility, scale-up and design aspects. To achieve a major turn with an enhanced synergy, refinements in the form of optimizing the co-ordination of the governing parameters of both the technologies (e.g., power, frequency, liquid height, electrode material, electrode size, electrode gap, applied voltage, current density etc.) have been validated. Besides, in order to supplement knowledge in the already existing pool, rigorous research on the past and present status has been done. Challenges were also identified and to overcome them, critical discussions covering an overview of the progressive developments on combining the two technologies and its major applications on pollutant degradation were conducted.

1. Introduction

Many researchers have placed ultrasonic–electrochemical (US/EC) mode of water treatment at a superior level over the conventional water treatment system as conventional methods involve only the transfer of contaminants from one media to another, creating the problem of secondary waste/sludge generation [1]. The advantage of conventional water remediation techniques has been mainly the low-cost, due to the employment of easily applicable methods like activated carbon (charcoal), filtration, coagulation, etc. However, these methods, though technically facile, has a high secondary waste disposal cost [2]. Besides, the use of alums, ferric salts or limes to coagulate contaminants is affordable, but they also require an extra process of disposing the obtained solid waste product. These problems are solved when energy based techniques like AOPs are employed [3]. Many processes of advanced oxidation techniques have been researched and are still continuing to get evaluated for the improvement of its application related to water purification. Among them US/EC is one of the latest technologies which is under rigorous study due to its favorable features such as mild operational condition, efficient functioning at room temperature and no additional requirement of chemicals [4]. Moreover, the main advantage of US/EC lies in the positive synergistic mechanism where irradiation of ultrasound (US) activates the electrode surface, accelerating the reaction process manifolds and hence, improving the current efficiency along with the system cost. More specifically, ultrasound improves the mass transport and reduces the diffusion layer thickness, consequently improving the efficacy of electrochemical (EC) processes. The main phenomena responsible in creating a mutual beneficial interrelationship between the two disciplines are US acoustic streaming, micro-streaming and turbulence due to cavitation and the formation of microjets in the course of the collapse of cavitation bubbles [5].

However, till date, the US/EC researches conducted are mostly on a laboratory scale, utilizing the conventional reactor configuration of the EC vessel and ultrasonic horns dipped in it. This type of configuration has been believed to be responsible for its sluggish evolution with lower reproducibility, scale-up and design aspects.

* Corresponding authors. Tel.: +91 22 414 5616; fax: +91 22 414 5614 (A.B. Pandit). Tel.: +82 2 3290 3318; fax: +82 2 928 7656 (J. Khim).
E-mail addresses: ab.pandit@ictmumbai.edu.in (A.B. Pandit), hyeong@korea.ac.kr (J. Khim).

http://dx.doi.org/10.1016/j.ultsonch.2015.05.015
1350-4177/

Nevertheless, it is still considered to be remarkable as various useful basic and encouraging results have been generated. A few groups have attempted to characterize lab-scale US reactors adapted as US/EC reactors, but the true optimization of such reactors requires contributions from many disciplines including physics, fundamental and applied electrochemistry, chemical engineering and material science [6].

In order to build up a novel design which can reproduce the spectacular effects generated at the laboratory scale, a detailed analysis and evaluation of the existing systems and the corresponding parameters are needed. Hence, an overview of the progressive developments on combining the two technologies was made first and its major applications with emphasis on pollutant degradation have been critically reviewed. Then, the review was focused on the existing research literatures collecting useful information on acoustic domain and its corresponding activities on the electrochemical processes, through which conclusive results are obtained to improve its possibility for environmental applications. Besides, detailed emphasis was given on the experimental and theoretical relation of various dependent/independent variables so that an optimized system can be designed efficiently. Brief study on the physical and chemical processes involved in pollutant oxidation during US/EC was also done in order to understand key advantages and disadvantages. The bottlenecks to be overcome for the full-scale application and various necessary future researches are also discussed. Overall, the major target is to provide enough necessary knowledge to facilitate the adoption of US/EC process as a new promising water treatment technology.

2. Brief history of sonoelectrochemistry

The collaborative study of US with EC dates back to 1934 when Moriguchi [7] tried decreasing the water decomposition voltage on a platinum electrode by insonation. Significant interest was generated during 1950s, with an electroplating of nickel and chromium under the assistance of US [8]. However, real applications on an analytical basis were reported mainly in the 1960s [9]. A little bit later, in the 1980s, Eren et al. and Osawa et al. started focusing on polymerization of styrenes [10] and thiophene [11] respectively, and also organic US/EC-synthesis [12]. One notable work in this field is that of Walton et al. creating the Kolbe EC-oxidation of cyclohexanecarboxylate in methanol as the mechanical switch in an EC-organic synthetic reaction [13]. On the contrary, Nonaka, Atobe et al. studied the EC-reduction of carbonyl compounds. His team, by manipulating the two-electron-per molecule monomeric alcohol under electrolysis and one-electron per molecule dimeric pinacol under sonication, generated the reverse mechanistic switch [14]. Since then, interest in US/EC has grown considerably as a result of the general enhancement in both EC and US equipment and methodology, exploring a wider range of experiments and a greater understanding of phenomena that lead to further comprehensive studies by several groups, including Compton et al. [15].

Increased attention on the US-mediated degradation of various organic contaminants, present both in natural and industrial water resources, has come into light since 1990s. This phase can be regarded as the approximate period from which peer-reviewed papers on environmental remediation using US/EC started originating [16,17]. In 1996, Trabelsi et al. analyzed the US/EC-oxidation of aqueous phenol solutions by applying the direct US/EC in the configuration named "electrode-apart-transducer" which can be considered as one of the pioneering works in the degradation field using this technology. In that study, 20 and 540 kHz at a constant current density of 6.8 mA cm^{-2} were used, with nickel foam as the cathode and platinized titanium grid as the anode. As a result, higher fractional conversions were obtained at both frequencies, but high frequency required shorter degradation time. At low frequency, the process was reported to be unrealistic due to the formation of toxic compounds such as quinones. Moreover, the combined technology was shown to be more efficient than the individual processes conducted separately [4]. Henceforth, the US/EC-oxidation of pollutants has been further practiced in the degradation of dye effluents such as Sandolan Yellow [18], Procion Blue [19], and Meldola Blue [20], of pesticides such as 2,4-dihydroxybenzoic acid [21], 2,4-dichlorophenol [22], and of additives such as thiosulfate [23] and cyanides [24].

Our research group focuses on the degradation of pharmaceutical compounds, pesticides, etc. using different approaches: (i) EC treatments; (ii) US treatments and (iii) US/EC treatments, as in the present study.

Table 1 shows the historical timeline of US/EC applied in various fields of scientific and engineering studies.

3. Applications of sonoelectrochemistry

The combination of an EC with a US field has been studied as an interesting way to generate highly reactive chemical species synergistically. The reason for the substantially enhanced synergy may be due to the combination of two supporting mechanisms. These benefits have been routinely highlighted in the literatures where several reviews summarize the different implementation of this discipline, hence intensifying its importance in a wide range of applications [43].

Some of the important applications of the combined US/EC technology are:

3.1. Sono-electrodeposition and sono-electroplating

It is the first documented application of US in the field of electrochemistry [8,44]. US/EC-deposition of the bioactive calcium phosphate coating [45] and CdSe films [46] have already been studied along with typical metallic deposits, such as silver oxide [47], silver [48] and tungsten [32]. Apart from scale-up study, other notable surface applications developed based on US/EC techniques are anodization [49], etching [50], US/EC-polymerization [51], US/EC-deposition [52] and composites electrode preparation [53].

3.2. Sonoelectroanalysis

Even though electroplating was documented first, but, US/EC-analysis resulted as a most popular field of academic studies. Increased sensitivity of the system, depassivation of the electrodes and faster degradation of the organic matrices are among the significant contribution of the US mechanistic outcomes of analytical procedures. The first literature on analysis is believed to be described by Allen Bard in 1963 [32], followed by the description of the mass transport effects of ultrasound by Kolb and Nyborg [54]. Since then, several reviews have extended the range of different analytical procedures used in the analysis of different chemicals in a wide range of matrices [55,56].

3.3. Sonoelectrosynthesis

Few researchers have reported literatures and review articles despite of receiving lesser attention as compared to other applications like US/EC-analysis. However, to synthetic electrochemists, the employment of US under thermostated condition is beneficial, not only due to faster rates of mass transport, but also due to

Table 1
Chronological timeline of sonoelectrochemical study.

Year	Event	Equipment/experimental condition	Important findings	Refs.
1934	Water electrolysis under US influence	Platinum working electrode	Under US irradiation water electrolysis took place at lower voltages, electrolysis rate is faster than normal (silent) conditions	[7]
1957	Sonically assisted electroplating (nickel and chromium)	Frequencies of 10 and 260 kc/sec	Same effects at both frequencies, depressed cathode polarization, slightly increased current efficiency, modified structural properties, decreased grain size, improved preferred orientation, improved hardness deposition, current densities over extended to higher values with the sound wave, decreased protection of porosity and corrosion, slightly improved adhesion and throwing power	[8]
1983	Diverse configurations and passivity of iron in sulfuric acid	Iron disks working electrode (diameter 3.8 cm, thickness of 0.16 cm) mounted on Plexiglas holder, 1.5 cm diameter exposed, 0.32 cm below plastic holder, wire soldered to disk's back for electrical contact, cell holder placed on rectangular Plexiglas tank of bottom area 15.2 × 53.3 cm^2, 17 cm deep electrolyte, 18 cm gauge platinum wire counter electrode, 25.4 cm long, ring shaped with 3.25 cm diameter, placed above iron disk, Hg/Hg_2SO_4 reference electrode placed 0.5 cm from the working electrode, rubber mat leached in 2 N H_2SO_4 on one end of the tank for good absorption, ultrasonic transducer co-axially gold-coated lead zirconate titanate ceramic spherical segment with a 5.08 cm diameter and 7.62 cm focal length, 1.58 MHz frequency	Curved piezoelectric transducer produced high frequency (1.58 MHz) US waves creating cavitation at the focal point, acoustic focal intensities generated up to 3.4 kW cm^{-2}, low frequency (20 kHz) US produced using exponential microhorn, depassivation produced at high focal intensities (above 1.5 kW cm^{-2}) with single (100 ms) pulse US, low intensities require continuous US exposure, induced depassivation followed by precipitation of a metal salt film upon metal surface before the oxide film formation	[23]
1993	Electrode cleaning, effects of high-intensity ultrasound on glassy carbon Electrodes	Glassy carbon cylindrical electrodes, about 2 mm long, sealed in epoxy resin, conventional electrochemical cells, Pt auxiliary and Ag/AgCl (3 M NaCl) reference electrodes, thermally jacketed by ethylene glycol coolant (12 °C), electrodes positioned parallel to the l/2 in diameter Ti horn tip, placed in the center of the cavitational plume US processor, power output level of 10 (120-pm peak tip amplitude), frequency 20 kHz, power 475 W, gap between Ti horn and glassy carbon electrodes 2 mm	Enhanced heterogeneous electron-transfer rates in dioxane, sonications in water gave no significant enhancement, surface roughness not changed appreciably after brief sonication in dioxane, except small amount of surface pitting, electrodes remained active for up to 5 days, prone to adsorb aromatic redox probes in aqueous media than polished electrodes, in water carbon surfaces are highly pitted, electroactive surface oxides density increased, kinetics improved after sonication in dioxane probably not associated with either increased microscopic electrode area or mediated electron transfer between surface oxides and solution analytes, but instead is likely to involve surface cleaning	[25]
1994	Voltammetry in the presence of US and surface effects	Three separate titanium tipped horn probes (13 mm diameter) extended by 127 mm, frequency 20 kHz, power up to 63 W cm^{-2}, thermostatted EC cell with copper cooling coil inserted in the solution, water circulated from a constant-temperature bath (within 2 °C), platinum microdisk electrodes with radii between 2.5 (±03) and 60.0 (±5.0) μm, platinum macroelectrodes of radii between 0.05 (±0.002) and 0.39 (±0.01) cm mounted on insulating Teflon sheath, polished using diamond lapping compounds to 0.25 μm, nickel electrode fabricated from a nickel wire with 1 mm diameter and 1.3 cm length utilized in Flade potential studies, electrode placed perpendicular to the axis of the horn at a distance of 30 (±5) mm, polished with diamond lapping compound to 0.25 μm	Flade potential for the passivation of nickel in air-saturated aqueous KOH solution anodically shifted in the presence of US, voltammetric study of $Cr(CO)_6$ in acetonitrile solution feasible without the passivation observed under silent conditions where the electrolysis results in surface-active species, adsorption of species blocks further electron transfer	[26]
1995	Electrically separated EC cell and US bath	Voltammetry of potassium ferrocyanide: two compartment cell, platinum wire anode (1 cm × 0.3 mm), platinum foil counter electrode (2 cm^2), saturated calomel reference (SCE) electrode, scan rates either 50 mV s^{-1} or 25 mV s^{-1}, for low frequency of 25 kHz: 24 W cm^{-2} fixed power output), liquid depth 15 cm, cell immersed, platinum electrode ~3 cm below liquid level; for high frequency bath of 800 kHz: power output variable approx. 18–61 W cm^2, cell fitted closely into the focused resonant cavity with electrode 4 cm below liquid level, constant temperature of 5 °C	Simultaneous application of US to representative solution-phase, production of step-shaped voltammogram at platinum electrodes of both 'macro' and 'micro' dimensions in reversible voltammetric couples, increased limiting current with US power, least affected by US frequency (20–800 kHz region), complex voltammetry of a platinized platinum electrode surface within the hydrogen adsorption regime in aqueous acid medium also least affected by sonication	[27]
	Penetration of sound waves in the glass wall of the EC reactor	Voltammetry of ferrocene: ultrasonic horn immersed in the solution (40 mm), electrode with radius 2.5 μm to 0.4 cm, three separate titanium tipped horn probes (diameter 13 mm) extended by 127 mm and operating at 20 kHz, power up to 63 W cm^{-2}, thermostatted electrochemical with copper cooling coil inserted in the solution		
1996	Bipotentiostatic control, titanium tip for EC system	Dried and argon saturated electrolyte solutions, US generator made of titanium full wave probe (for media with low surface tension), 13 mm	Detection of one very broad reduction wave at more negative potential, may be due to a passive layer on the titanium surface which allows only sluggish	[28]

Table 1 (*continued*)

Year	Event	Equipment/experimental condition	Important findings	Refs.
		diameter, 20 kHz sound frequency, power of up to 80 W cm^{-2}, thermostatted cell (25 ± 2 °C), Pt disc working electrode, 1 mm diameter, graphite rod counter electrode, saturated calomel reference electrode, titanium alloy immersion horn with tip placed opposite to a disc shaped working electrode which is oriented parallel (or perpendicular) to the vibrating horn tip, titanium horn electrically earthed	electron transfer, detection of extremely high limiting currents at sufficiently negative potentials with US	
	US horn tip used as working electrode (sonotrode)	Two sonotrode design: (1) titanium tip, 20 kHz sonic horn as working electrode, potentiostat mode connected through graphite rod touching the horn, (2) 0.15 cm Pt disc fitted into a tailored hole in the Ti tip using Araldiate and insulated to act as an alternative working electrode, disc connected by wire through a hole drilled into the side of the tip, in both types of sonotrode the body of the horn insulated from the solution by means of a Teflon sheath and thermostatted the cell obtained using stainless steel cooling coil inserted in the solution, working electrodes (Ti horn tips or Pt disc inserts) polished using diamond lapping compounds to 0.25 μm, three electrode potentiostat mode, carbon rod counter electrode, saturated calomel reference electrode, dried acetonitrile or water purified with resistivity 18 MΩ as background electrolyte	Untreated Ti alloy tip sonotrode gave behavior characteristic of the n-type semiconducting layer of TiO, known to be present on the surface of metallic titanium, Platinum disc embedded in the titanium alloy tip of the horn probe gave high mass transport conditions and clean reversible electrochemistry for a variety of model systems	[29]
1997	Development of fundamental and applied aspects of US/EC	Baths and immersion horn probes as two major sources of US, piezo driven transducers limited to one frequency, often 20 kHz; three-electrode cell with an immersion horn incorporated in the center, well-thermostated to within ±2 °C, US horn immersed in solution and above working electrode, bipotentiostat with one working electrode connected to earth	Both physical and chemical processes involved, US affects through mass transport and thermal, use of multiphase systems and the detection of radical intermediates or real chemical effects of US remain largely unexplored, mixing or homogenization effect of power US drastically affects systems with more than one phase (gas–liquid, liquid–liquid or solid–liquid) and the rapid transport in the bulk phase due to turbulent convection, ideally suited for the development of the paired electrosynthesis, high energy liquid jets of some 100 ms^{-1} impinging onto the electrode surface due to cavitational collapses near the electrode surface	[15]
1998	Mass transport enhancement by violent collapse of bubbles and shock waves in sonovoltammetry with hydrodynamic modulation from US	Potentiostat mode, Pt disk working electrode (1.6 mm diameter), polished with diamond paste followed by alumina to 0.3 μm, lead-zirconate-titanate (PZT) transducer driven, 20 kHz frequency, 475 W output power, PZT transducer coupled to titanium horn immersed in EC solution, standard macrotip (11 × 13 mm) with maximum amplitude of 120 μm, directly immersed sonicator horn with face immediately opposite and parallel to the working electrode surface, constant temperature of 22 ± 1 °C, Ag/AgCl reference electrode for aqueous experiments, Ag/Ag for nonaqueous work, separated from the working electrolyte by a fine-porosity glass frit, Pt wire as auxiliary electrode, argon-saturated solutions to remove oxygen	Hydrodynamically modulated mass transport by US in EC due to combination of field-induced fluid motion driven at the frequency of the US and from the effects of acoustic cavitation observed in both aqueous and nonaqueous media, larger AC signal with increased cavitational activity, and a signal that is primarily driven at the US frequency results from field-induced motion occurred, current signal contains a time-independent DC component as well as a time-dependent AC component, DC signal arises from steady forces, primarily acoustic streaming, AC signal resulted due to combination of US field induced fluid motion and cavitational effects, DC component assumed to result from acoustic streaming but may be affected by the intensity of cavitation	[30]
	Diuron (herbicide) degradation using glassy carbon and BDD electrodes	Cyclic voltammetry and bulk electrolysis in 1:1 methanol:water solution with K_2SO_4 as supporting electrolyte, undivided cell in former case and H-type cell in the latter case with separate compartments using glass frits, potentiostat mode, glassy carbon disc anode (area 0.07 cm^2) for CV, glassy carbon plate (28 × 13 × 2 mm^3) in bulk electrolysis, silver wire and a platinum gauze as reference and counter electrodes, respectively, two sources of low-frequencies US, i.e. a cleaning bath with 35 kHz and 160 W, and a horn (area 1.0 cm^2) of titanium alloy with 20 kHz and power density 6 W cm^{-2}, horn immersed in glass finger to attain electrical isolation from the solution, water flowing through this finger serves both as a cooling agent and as a coupling medium for transfer of US from the horn into the cell, finger with the horn immersed in anodic compartment (70 ml) of the H-type cell, 1–4 atm overpressured cooling water	Major oxidation isolated with 23% yield from the loss of one electron and one proton with formation of a nitrogen radical and of the corresponding N–N dimer, two more compounds isolated with 12% and 10% yields suggested to originate from an intramolecular Fries rearrangement, i.e. migration of an amide group from a monomeric unit of the dimer to the aromatic ring of the second one, with formation of a dichloro–*N*, *N*–dimethyl benzamide derivative, several non-identified minor compounds also generated which could involve multi-electron oxidation processes since the overall oxidation process of diuron required more than one electron	[31]
1999	Tungsten-supported boron-doped CVD diamond electrodes under US/EC	Cylindrical tungsten substrates (5 mm diameter, 5 mm height), BDD electrodes mounted on Teflon holders by heat-shrink procedure, electrical connection by spot-welding a nickel contact to the reverse side of the tungsten substrate, potentiostat mode, thick gold wire counter electrode,	Highly boron-doped (atomic concentration 1020–1021 cm^{-3}) conductive diamond films deposited on tungsten substrates by hot-filament assisted chemical vapor deposition from a gaseous feed of methane and diborane in hydrogen, standard rate constant for electron transfer is 3×10^{-3} cm s^{-1}, EC	[32]

(*continued on next page*)

Table 1 (*continued*)

Year	Event	Equipment/experimental condition	Important findings	Refs.
		saturated calomel reference electrode, argon degassed solution, mixture of KCl, orthophosphoric acid, NaOH and ultrahigh quality water of a resistivity not less than 18 MΩ cm as electrolyte, 20 ± 2 °C constant temperature	processes at 90 W cm^{-2}, sonication without significant electrode deterioration, surface property changed due anodic polarization, increased current after negative polarization, voltammograms under US conditions suggested potential pretreatment with possible process switching from nearly mass-transport controlled to virtually absent mass transport	
	Depassivation of electrode by ultrasound	250 cm^3 working volume cell, 25 ± 2 °C constant temperature, BDD anode (5 × 5 mm^3), mounted on Teflon, coiled platinum wire counter electrode, saturated calomel reference electrode, electrical connection to the rear (graphite) side via a brass rod attached using silver epoxy resin, the rear of electrode assembly enclosed using a sealant-wax, whole unit placed near the bottom of the cell, directly opposite from 13 mm diameter titanium tip of a US horn, frequency 20 kHz, US intensity 14 W cm^{-2}, elimination of bipotentiometric control of titanium horn by insulating the transducer from probe with Teflon disk, 10 mm gap between transducer probe and working electrode	US assisted cathodic stripping voltammetry at BDD electrode for detection of lead, concentrations above 3 mM, linear sweep voltammetry gave analytical signal from a cathodic strip of electrodeposited PbO_2, linearity observed from 3 ± 100 mM, lower detection limit 3 mM, square-wave voltammetry to lower the detection limits with linearity of the order of 10^{-8} M	[33]
2001	Heavy metal determination analysis	Working electrode face on to US horn with a gap of 5 mm, horn equipped with a titanium alloy microtip (diameter 3 mm), 20 kHz frequency, power intensity 200 ± 5 W cm^{-2}, thermostatted with stainless steel cooling coil inserted, temperature 25 ± 3 °C, bipotentiometric control of the titanium horn by insulating the transducer from the probe with a thin Teflon disk and connecting with a screw, 3 mm diameter glassy carbon disk electrode plated in situ with mercury from a 1 mM solution, polished using diamond lapping compounds to 0.1 mm, saturated calomel reference electrode, 20 cm coiled platinum wire counter electrode	Enhanced mass transport to the electrode surface and cavitational depassivation maintaining surface activation during preconcentration, good intrasample reproducibility and favorable with independent analysis of the mucous extract by electro-thermal atomic absorption spectroscopy, theoretical detection limit of 0.004 ppm determined, sonoelectroanalysis facilitates the use of a nondestructive biomarker for the detection of heavy metals with the following advantages: minimal experimental procedure, elimination of sample pretreatment, possibility for portable apparatus and relative inexpense compared with either ICPAES or AAS giving it the potential to become a powerful and useful field apparatus	[34]
	Reactive dye Procion Blue degradation	250 ml cell, BDD films deposited tungsten wires as working electrode (1 mm diameter, 10 mm length), platinum counter electrode, saturated calomel reference electrode, working electrode fitted into Teflon holder and placed at the cell's bottom, frequency 24 Hz, power 200 W, maximum intensity 30 W cm^{-2}, 13-mm-diameter glass horn, phosphate buffer solutions prepared from deionized water (resistivity 18 MΩ cm), degassed with argon	Direct partial oxidation with four electron transfer under solvent window up to 2.5 V vs. SCE in PBS (pH 2), extensive degradation of Procion Blue does not occur at potentials below the required one for solvent decomposition, oxidation most easily achieved in acidic solution and at low dye concentrations, electrode surface fouling noted under alkaline pH and at higher dye concentrations, influence redox processes which are directly associated with defect sites on the diamond electrode itself	[35]
2003	N,N-dimethyl-p-nitrosoaniline degradation	Conventional three-electrode arrangement, potentiostat mode, free-standing 2 mm × 5 mm polycrystalline BDD electrodes rich in graphitic impurity states and grown in house on tungsten rod substrates (1 mm diameter, 10 mm length) as working electrode, platinum coil counter electrode, saturated calomel reference electrode, frequency 24 kHz, output power approximately 8 W cm^{-2}, 13 mm diameter glass horn	US power drastically improves bleaching rate by increasing the rate of mass transport at the electrode-solution interface, initially more efficient bleaching process using BDD electrodes rich in sp^2 carbon impurity states, appearance of reactive intermediates such as hydroxyl radicals preferentially in the vicinity of impurity states, mass transport dominated in controlling the efficiency of bleaching process	[36]
2007	Sonovoltammetric determination of 4-nitrophenol on diamond electrodes	Three electrode arrangement with one-compartment Pyrex glass cell (50 mL), N_2 degassing, BDD films with 8000 ppm boron content as working electrode, exposed area 0.25 cm^2, Ag/AgCl (3.0 mol L^{-1} KCl) reference electrode, 1 cm^2 Pt foil counter electrode, US horn tip placed in front of working electrode, computer controlled potentiostat, bipotentiostatic control of the titanium horn tip with insulated transducer from the probe using Teflon disk, 20 kHz frequency, 20% and 40% power intensity, amplitude 20%, acoustic power 14 W, acoustic energy transferred 155 and 178 J for oxidation and reduction processes of 4-nitrophenol on the diamond electrode, respectively, supporting electrolyte is Britton-Robinson 0.1 mol L^{-1}, pH 6.0 adjusted using NaOH 1.0 mol L^{-1}	Significant improvements in the analytical sensibility observed due to electrode surface cleaning and the enhancement in the transport of species to the electrode surface provided by US, limit of detection for oxidation and reduction processes diminished from 11.7 to 3.87 and from 6.38 to 2.57 μg L^{-1}, respectively	[37]
2008	Phenols degradation	Cylindrical single-compartment cell, BDD or Pt anode with 24 cm^2 immersed area as working electrode, titanium foil with same area as cathode, interelectrode gap 1 cm, current density 20 mA cm^2, pH 3.0 adjusted with 0.2 M H_2SO_4, 200 cm^3 phenol sample volume, 10 °C constant temperature, solution volume 200 cm^3, frequency 33 kHz, power 50 W	With US, for BDD, increased degradation rate and current efficiency are 301% and 100%, respectively, for Pt 51% and 49%, respectively, increased diffusion coefficient for BDD and Pt are 375% and 42%, respectively, US effect on BDD much greater than for Pt, without US large adsorption of phenol on both electrodes, with US, the adsorption amount decreased by 79% and 56% on BDD and Pt electrodes, respectively, renewal and activation effect of US	[38]

Table 1 (*continued*)

Year	Event	Equipment/experimental condition	Important findings	Refs.
			on the surface of BDD more obvious than Pt, enhancement for EC by US on BDD is 108% and for Pt is only 25%, degradation of phenol on BDD easier than Pt, lower amount of intermediates produced at BDD than Pt	
2009	Methylparathion determination in potato and corn extracts 4-Nitrophenol degradation in lemon and orange juices	50 mL one compartment pyrex glass cell with three electrode arrangement, N_2 degassing, BDD films with 8000 ppm boron content working electrode (0.25 cm^2 area), Ag/AgCl (3.0 mol^{-1}KCl) reference electrode, 1 cm^2 Pt foil counter electrode, US horn tip placed in front of working electrode face (gap 5 mm), computer-controlled potentiostat mode, bipotentiostatic control of titanium horn tip, insulated transducer from the probe with Teflon disk, Britton-Robinson (BR) 0.1 mol L^{-1} buffer optimized at pH 7.0 for methylparathion and at pH 6.0 for 4-nitrophenol as supporting electrolyte. 20% US intensity, 14 W power, 20 kHz frequency	Detection limit for methylparathion in water and corn extract were 4.86 and 10.1 μg L^{-1}, respectively, 55% and 72% lower than silent voltammetry, 83.5% and 96.2% recovery values, possible reasons are electrode surface cleaning and mass transport enhancement toward the electrode surface	[39]
2010	Voltammetric scale up to pre-pilot stage using trichloroacetic acid (TCAA)	Laboratory glass sonochemical reactor (adapted as sonoelectrochemical device) used for bulk electrolysis in batch mode, galvanostat (120 mA_13.4 V maxima power), catholyte volume 200 mL, for divided mode, a Nafion 450 cationic membrane to separate catholyte and anolyte chambers, with anolyte volume 200 mL, for non-optimized flow-sonoelectrochemical system used for the scale-up of the process, polypropylene reactor designed for divided and undivided configuration, catholyte and anolyte volume 2000 and 1000 mL, respectively, titanium disk with d = 4 mm, 0.126 cm^2 and spiral wound platinum wire cathode for voltammetric experiments, for bulk electrolyses, mesh-plate of Ti with 2 cm^2 of active area in each electrode face in the batch cell and 20.0 cm^2 in the flow cell used as cathodic material and platinized titanium (Pt/Ti) mesh with 20 cm^2 as anodic material in both scales, reference electrode is an Ag/AgCl/KCl (3 M), supporting electrolyte Na_2SO_4 purged with argon to avoid oxygen entrance, frequency 358,850,863 kHz, power 0.039, 0.047, 0.054 W	US alone gave poor performance compared to US/EC, batch scale US/EC analyses with horn-transducer 24 kHz positioned at about 3 cm from the electrode surface achieved little degradation, but specifically designed US/EC reactor (not optimized) during the scale-up provided better results (fractional conversion 97%, degradation efficiency 26%, selectivity 0.92 and current efficiency 8%) at lower ultrasonic intensities and volumetric flow	[40]
	Substituted phenols degradation at low-frequency (40 kHz)	Constant current density (20 mA cm^{-2}), room temperature (25 °C), 250 mL electrolyte (1 mM substrate + 0.2 M Na_2SO_4), magnetically stirring for EC, frequency 40 kHz, power 150 W, BDD or PbO_2 anode with 4 cm^2 geometric area, same sized stainless steel sheet cathode, electrode gap 10 mm	Enhancement more obvious at BDD anodes than at PbO_2 anodes, at BDD anode, 73–83% disappearance of p-substituted phenol and 60–70% for COD removal, for PbO_2 anode, 50–70% disappearance of p-substituted phenols and only 5–25% for COD removal, different enhancement extent due to diverse effects of ultrasound on specialized types of hydroxyl radicals, hydroxyl radicals free at the BDD electrodes with a larger reaction zone whereas adsorbed at the PbO_2 electrodes with a smaller reaction zone	[41]
2011	Un-hydrolyzed/hydrolyzed reactive blue (RB) 19 dye degradation	Perspex sheet undivided electrolytic cell, lead oxide working electrode (14 × 15 cm^2), stainless mesh steel counter electrode, working and counter electrode positioned vertically and parallel to each other with gap 2.5 cm, DC power supply, Digital Ultrasonic Bath, frequencies 20–80 kHz, pH 3–9 controlled using 1 M NaOH or 1 M HCl	90% color removal, 56% TOC removal at frequency 80 kHz, pH 8 after 120 min, un-hydrolyzed RB 19 dye formed acetic acid, benzoic acid etc. after 30 minutes with the complete removal of dye, for hydrolyzed dye, 10 min was enough, first order kinetics, US/EC better than individual processes, total energy consumption reduced to half	[42]
Present	General US/EC, US/EC-oxidation, optimization, organic synthesis	–	–	

electrode activation: the cavitational phenomenon can clean or passivate surfaces and lead to the possibility of in situ electrode activation. A further advantage is that the product distributions may be changed upon the application of US.

So far, a specific and targeted study of US/EC-synthesis under monophasic condition has been conducted [57]. However, in the case of biphasic media, sonication results in the formation of an in situ emulsion, initiated by cavitation events at the liquid/liquid interface, with a droplet size of ca. 1 μm with mean particle size of 0.2–2.0 μm, and a size distribution range of 0.1–10 μm or even narrower [58]. System parameters such as ultrasonic power, the reactor geometry and the chemical composition determine the degree of this acoustic emulsification process [57].

Among the successful syntheses using US/EC, nanoparticles of different materials can be mentioned. Various particles like copper [59], magnesium [60], tungsten [61], gold [62], silver [63] and few alloys etc. are produced cathodically. Some productions require the follow up process of precipitation or using metal foils as sacrificing anodes.

3.4. Environmental remediation

One of the justifiable and successful approaches has been in the application of the degradation of pollutants through both the reduction and oxidation processes. Both the processes can be carried out at the same time in different regions of the reactor, and with the same operating cost. One more remarkable feature is that the system can be operated without utilizing harmful reagents while treating wastewater making it environmentally benign.

The present review deals mainly with the remediation of pollutants and detailed explanations are given in the follow up sections.

4. Advantages of US/EC on environmental application study

It is clear that there are contradictory results of degradation of refractory compounds using conventional treatment like a biological process due to its high chemical and physical resistance [64]. Many researchers have reported that the advanced oxidation processes, including US and EC-oxidation, are significantly useful for cleaning biologically toxic or non-degradable materials such as aromatics, pesticides, petroleum constituents, and volatile organic compounds in wastewater [65]. By introducing such system, the contaminant materials are converted to a large extent into stable inorganic compounds such as water, carbon dioxide and salts, i.e. they undergo mineralization through series of chemical reactions. This is possible due to the generation of highly reactive and unstable hydroxyl radicals. These radicals have a high oxidation potential of 2.80 V and degrades the pollutants nonspecifically [43]. When US is irradiated to water, the same reactive radical is produced through Eq. (1):

$$H_2O+))) \rightarrow \cdot H + \cdot OH \quad (1)$$

In the case of EC process, hydroxyl radical generation takes place through Eq. (2),

$$M + H_2O+))) + M(\cdot OH) + H^+ + e^- \quad (2)$$

where M is the electrode material and M(·OH) is the heterogeneous hydroxyl radicals adsorbed in the anode. Supplementary reactive radicals with potential oxidizing property can also be generated according to the Eq. (3) given below:

$$M(\cdot OH) + R \rightarrow mCO_2 + nH_2O + H^+ + e^- \quad (3)$$

However, separate processing of these methods is not as efficient as their combined technology [66].

In the case of US irradiation, the process of bubble formation and other important physical phenomena like acoustic streaming show major contribution to the combined process. At the electrode–solution interface, the occurrence of crevices and active sites help in forming gas bubbles readily [67]. Besides, due to the weaker molecular interactions at the solid/solution interface, cavitation occurs more readily as compared to the bulk solution. Here, strong physical phenomena such as macroscopic turbulent streaming and cavitation/microstreaming also dominate. These physical impacts, including microjet and acoustic streaming generated under the influence of various parameters including ultrasonic power, frequency and solution phenomena such as viscosity, volatility, the presence of the nucleation site, etc. help in decreasing the diffusion-layer thickness of the electrolysis system to less than 1 mm, and activating the electrode surfaces enhancing mass transfer and EC current [68]. They are also responsible for reactivating the fouled electrode, thereby leading to enhanced degradation efficiencies [21,69]. These are the main mechanisms of US utilized in the US/EC system to increase the degradation efficiency of toxic compounds.

US/EC itself presents several innovative aspects as: (i) toxic pollutants in a wide range of concentration can be destroyed without the use of high temperature and pressure [70], (ii) the technology is environmentally friendly since it avoids the emission of gases and the use of any chemical [71] and (iii) only electricity is used as a reactant [72]. In spite of the advantages of this hybrid process, not many environmental applications of this integrated alternative have been reported in the literature.

It is widely accepted that the degradation of the pollutants or the enhancement of other oxidation processes by the US is due to its cavitation, which can cause physical and chemical effects. US with low frequency usually brings physical effect which can clean electrode surface and improve mass transport, while US with high frequency usually brings chemical effect which can produce active substances such as hydroxyl free radicals [73]. All these investigations have made a valuable understanding of cavitation and its promotion of the efficiency of this combined technology.

However, we consider that it is necessary to explore the mechanism of enhancement by US from a more fundamental aspect of electrochemical oxidation (EC process): effects of material and electrochemical characters of electrodes in US/EC process. In fact, degradation of pollutants by EC oxidation at electrode surface is complex, which involves the following three steps: (a) mass transport process: the diffusion of pollutants from bulk to electrode surface; (b) adsorption and desorption: the adsorption of pollutants near the electrode to electrode surface and desorption of intermediates from the electrode surface; and (c) EC reaction: the oxidation reaction of pollutants by losing electrons (with two pathways: direct oxidation and indirect oxidation pathway). More detailed explanation is given in the next section. The intensity and the rates of the three steps may differ with different electrode materials, at the same time, the reaction pathway and intermediates formed may also be not same. Therefore, it is necessary to investigate these aspects too, in order to understand the US-enhanced EC oxidation.

5. Fundamental mechanism of combined US and EC

The absorption of power or energy intensity by solution generates a significant movement which is actually induced by the kinetic energy transformed from acoustic energy in the bulk. This field movement of fluid displacement is created when ultrasound passes electrolysis through a solution. Besides, there can be increased in current too if the electrode is closed enough to the ultrasound generation due to the recurrent movement and

transport of solution species. Technically, when electrode surface is placed sufficiently closed to ultrasonic transducer, cavitation bubbles undergo asymmetrical implosion near it (Fig. 2). This then produces a strong microjet of liquid and violent shock waves which can induce erosion and cleaning of the electrode surface. Consequently, due to the strong mechanical forces of US waves, the species adsorbed at electrode can be easily desorbed, speeding up the electron transfers at the electrode region and mass transfer toward the bulk and vice versa [74,75]. Hence, the fast transient movements caused by microjet and acoustic streaming can speed up the solution mixing dramatically.

Quantitatively, the mass transport induced by US toward the electrode and back to the bulk can be calculated through diffusion layer thickness variation. The equation is:

$$I_{\text{lim}} = \frac{nFDAC_{\text{bulk}}}{\partial} \tag{4}$$

where I_{lim} is the limiting current, n the number of electron transferred, F is the Faraday constant, D is the diffusion layer, A is the electrode area, C is the concentration of the bulk solution. The constant ∂ is a function of diffusion coefficient, D and both the parameters are associated through the relation, $\partial(D) = Dx$. Holt et al. and Compton et al. have already reported it as an index for mass transport process with dependence on applied US power and electrode radius. Compton et al. has further revealed the appreciably lowered value of ∂ in the presence of US, indicating it to be a function of mass transport [76,29]. However, in some cases, when the electrode is sufficiently placed near the transducer, the high impact physical forces of microjet and cavitation can deteriorate the electrode surface. Till now researches have claimed about the electrode cleaning and corresponding performance enhancement due to these forces, however studies on the changes in electrode surface cannot be denied either. This may be one good reason for the minimum reports of application of synthesized electrodes on US/EC oxidation of pollutants. In the tables enclosed with the manuscript, especially Table 1, many recorded researches citing the benefit of mass transfer induced by US have been mentioned.

While adsorption-desorption and electron-mass transfer occur simultaneously, side by side, the direct and indirect mechanisms can be partly regarded as the consequences of the above mentioned mechanisms. Direct mechanism is claimed to be occurred at the electrode surface with hydroxyl as the main reactive radical, indicating that the pollutant should somehow be in contact with the electrode. However, recently, it has been suggested that the direct degradation reaction site is not only confined to electrode surface, but also in the vicinity of the electrode. Nevertheless, the mechanism is possible only when pollutant species are adsorbed or transported toward the electrode. The examination of the direct electrochemical degradation of pollutants has been reported to be initiated from eighties by altering the anode materials. However, so far in the reported cases of US/EC-oxidation of pollutants, no researches have scientifically studied on the direct mechanism of the pollutant degradation. One probable reason for this may be that the application of this combined technology on degradation of pollutant is still in infant stage. However, many published articles on the direct oxidation of pollutants at the anode using only EC can be found. A thorough review on it has been done by Carlos et al., recently [77]. This group has clearly mentioned on indirect oxidation as well. In the indirect degradation mechanism, there involve a mediator radical mainly in the form of electrolyte and the main reaction site is usually the bulk area. From this point of view, all the sonoelectro-oxidation of pollutants reported in this review paper can perhaps be concluded as indirect since all of them have employ electrolytes. However, according to the same group, direct oxidation has been claimed as the degradation of pollutant using hydroxyl radical generated in-situ, as far as wastewater is concerned there should be production of this hydroxyl radical. Hence, there can be a possibility of both direct and indirect oxidations occurring simultaneously. Nevertheless more study on it is recommended for a concrete affirmation.

6. Combination of US/EC with other techniques

Till date, published works on the adoption of other degradation techniques to combine and upgrade the US/EC system are still countable. Among them, the application of Fenton process by utilizing iron electrode material itself or by the addition of external iron is popular and has been proved to be highly competent. On the other hand, littlest work on the adoption of other approaches like UV and ozone can be found. A summary on the extended works of US/EC is compiled up as Table 2.

The basic mechanisms that bind these different techniques in one platform can be known from the following explanations. ·OH radical, produced by the expansion and rapid adiabatic compression or collapse of the cavitation bubbles, tends to recombine into H_2O_2. This sonochemically generated H_2O_2 alone is not able to react and degrade the target molecule. On the other hand, in situ generation of H_2O_2 using electrochemical techniques has been extensively studied for the destruction of organic pollutants. In acidic solution, H_2O_2 is electrochemically produced by a two-electron reduction of molecular oxygen at the cathode surface [78].

$$O_2 + 2H^+ + 2e^- \rightarrow H_2O_2 \tag{5}$$

However, hydrogen peroxide generated through cavitation action or electrochemical reduction of molecular oxygen is not highly active toward the destruction of an organic species. Hence, in order to circumvent this problem, various researches have employed Fenton's reagent system enabling to generate maximum amount of free radicals (specifically hydroxyl radicals). Fenton system can be created either by adding Fe^{2+} to the solution or selecting iron as electrode material. This is known to catalyze the destruction of organic material through the generation of extra hydroxyl radicals, according to the reaction given below [22]:

$$Fe^{2+} + H_2O_2 \rightarrow Fe^{3+} + OH^- + OH^{\cdot} \tag{6}$$

Few studies on the combination of US/EC and Fenton have been reported already. Abdelsalam et al. studied the degradation of an organic dye molecule, Meldola Blue, under the influence of US power and in combination with electrochemically-generated hydrogen peroxide. A novel flow system has been used to measure the degradation as a function of time with minimum disturbance to the acoustics of the US/EC reactor. The effect of adding Fe^{2+} to the rate of dye degradation is shown to be significant. Under optimum conditions the rate constant for dye degradation was found to reach a maximum value of $(23.7 \times 0.35) \times 10^{-3}$ min^{-1} assuming pseudo-first order kinetics. The rate constant for the complete destruction of MDB, determined by chemical oxygen demand, was found to be significantly slower at $(10.2 \times 2.6) \times 10^{-3}$ min^{-1} [79].

Yasman et al. also reported the combination of US waves, EC and Fenton's reagent as a new method for the detoxification of hydrophilic chloroorganic pollutants: the common herbicide 2,4-dichlorophenoxyacetic acid (2,4-D) and its derivative 2,4-dichlorophenol (2,4-DCP) in effluent water. The high degradation power has been credited to the large production of oxidizing hydroxyl radicals and high mass transfer due to sonication. Half of the 2,4-D solution (300 ppm, 1.2 mM) was degraded within 1 minute using the combined US/EC-Fenton treatment (at 20 kHz) with a very small current density. When treated for 600 s, full degradation of the herbicide with sizable oxidation of 2,4-DCP

Table 2
Sonoelectrochemical degradation in association with different methods.

	Pollutant	Methodology	Equipment/experimental conditions	Important findings	Refs.
1	Meldola Blue (dye)	US/EC-Fenton	Thermostatted glass cylindrical cell (diameter 5.8, height 12 cm), piezoelectric transducer, frequency 27 kHz, voltage amplitude 100 V, constant temperature 25 °C, reticulated vitreous carbon electrode (15 mm × 10 mm × 5 mm), platinum gauze counter electrode, silver wire pseudo-reference electrode, electrodes fixed on cell wall to minimize acoustic disturbance within the sonochemical reactor	Enhanced degradation by Fe^{2+}, EC generated H_2O_2, maximum degradation of $(23.7 \pm 0.35) \times 10^{-3}$ min^{-1} at optimized condition, pseudo-first order kinetics, COD removal significantly slower with $(10.2 \pm 2.6) \times 10^{-3}$ min^{-1}, Fe^{2+} optimum concentration in the range of 0.5–1 mmol dm^{-3}, optimum frequency range between 123 and 126 kHz	[79]
2	2,4-Dichlorophenoxyacetic acid (2,4-D) 2,4-Dichlorophenol (2,4-DCP) (herbicide)	US/EC-Fenton	Glass cylinder vessel reactor with internal diameter 25 mm, effective sample volume 10 mL, solution temperature 25 ± 1 °C, double jacket cooling array circulated, horn type sonication via titanium alloy tip (13 mm in diameter) dipped in from the top of the reactor, nickle foil working and counter electrodes (125 mm thin, 11 mm radius, 20 mm height), placed around a horn with 11 mm radius, galvanostatic mode of operation, current intensities not exceeding 100 mA, supporting electrolyte Na_2SO_4, power 75 W, frequency 20 kHz	50% oxidation of 2,4-D solution (300 ppm, 1.2 mM) in 60 s, full degradation in 600 s, US/EC-Fenton degradation efficiency higher than US/EC, shorter degradation time, optimum concentration of Fe^{2+} ions about 2 mM	[22]
3	4,6-Dinitro-o-cresol (DNOC) 2,4-Dichlorophenoxyacetic acid (2,4-D) (herbicide) Azobenzene (dye)	US/EC-Fenton	250 mL open, cylindrical and undivided glass cell (6 cm diameter), temperature 25 °C, cylindrical Pt mesh anode (area 4.5 cm^2) placed in the center, carbon-felt cathode (15 cm × 8 cm) covering the inner wall of the cell and surrounding anode, H_2O_2 produced from reduction of O_2 dissolved in the solution, rate of continuous supply of saturation gas 1 l min^{-1}, 250 ml sample volume, 0.05 M Na_2SO_4 background electrolyte, 0.1 mM Fe^{3+} as catalyst, pH 3.0 adjusted with H_2SO_4, galvanostatic mode with 200 mA, US irradiation at low (28 kHz) and high (460 kHz) frequencies, ceramic piezoelectric transducer placed below the cell, US output power 20, 60 and 80 W	Destruction of the herbicides 4,6-dinitro-o-cresol (DNOC) and 2,4-dichlorophenoxyacetic acid (2,4-D) significantly accelerated, no improvement observed for dye azobenzene (AB) degradation, nature of organic structure plays an important role, lowest US power (i.e., 20 W) more effective than higher power	[80]
4	Phenol	US/EC-Fenton	5 L reactor, piezo-electric transducer, frequency 34 kHz, power 120 W, stainless steel anode and cathode of equal dimensions (5 cm × 5 cm × 0.5 cm), continuously magnetic stirring, no pH control, ionic strength maintained using 1000 mg/L Na_2SO_4, compressed air supply for internal production of H_2O_2, constant temperature	Phenol degradation strongly dependant on Fe^{2+} concentration, H_2O_2 concentration, initial phenol concentration, current density and solution pH, optimum electrode distance 5 cm, Fe^{2+} dosage 4 mg/L, H_2O_2 concentration 500 mg/L, initial pH 3 and current density 12 mA/cm^2, first order kinetic, kinetic rate constants at optimum operating conditions are 0.0067, 0.0286, 0.0683 min^{-1} for Fenton, electro-Fenton, sono-electro-Fenton processes, respectively	[81]
5	Cationic red X-GRL	US/EC-Fenton	Open, undivided glass vessel (dimension 130 mm × 80 mm × 170 mm), 1 L sample volume, temperature 27 ± 1 °C, activated carbon fiber cathode with dimension 100 mm × 90 mm, same geometrical working area RuO_2/Ti mesh anode, installed parallel, electrode gap 50 mm, ultrasonic horn dipped into the solution between cathode and anode, effective depth 20 mm, air supply rate 450 cm^3/min, galvanostatic mode	Pseudo-first-order model, apparent rate constant 0.021 min^{-1} (R^2 = 0.9982) in electro-fenton process, 0.0245 min^{-1} (R^2 = 0.996), 0.027 (R^2 = 0.9956) and 0.0326 min^{-1} (R^2 = 0.995) in the sonoelectro Fenton process with 80, 120 and 160 W, respectively. Apparent rate constant rapidly increased with US irradiation into the electro Fenton system, also higher with increased ultrasonic power	[82]
6	Azure B dye	US/EC-Fenton	0.5 L volume chemical reactor for Fenton process, 1.5 L volume sono-reactor with recirculation for sonolysis, three electrode cell with jacketed stainless steel cylindrical ultrasound cell, temperature 25 ± 3 °C, US probe of 13 mm diameter, power input 91 W, frequency 24 kHz, oxygen fed, reticulated vitreous carbon cathode (4 cm × 4 cm × 0.5 cm), platinum gauze counter electrode, saturated calomel reference electrode	First-order kinetics, highest degradation obtained at pH between 2.6 and 3, rate constant followed US/EC-Fenton > Fenton > US, rate constant by sUS/EC-Fenton is ~10-fold that of US alone and ~2-fold the one obtained by Fenton under silent conditions, COD removal ~68% and ~85% by Fenton and US/EC-Fenton respectively, achieving AB concentration removal over 90% with both processes	[83]
7	C.I. Reactive Black 5	US/EC-Fenton	500 mL pyrex-glass reactor, cast iron plates as anode and cathode (85 mm × 20 mm × 3 mm), electrode gap 25 mm, 65 mm into the solution, mixing speed 150 rpm, 15 min reaction, pH 7.5, ferric iron $Fe(OH)_3$) flocs at 30 rpm for 3 min, low frequency 35 kHz, power applied 80 W	Optimal conditions with initial pH 3, DC current 0.25 A, H_2O_2 dosage 800 mg/L and electrode distance 2.5 cm for both EC-Fenton and US assisted EC-Fenton processes, oxidation in two stages: a rapid oxidation stage in the first 2.5 min and a slow stage for the remaining part of oxidation time, the oxidation rate and efficiency of US/EC-Fenton process higher than EC-Fenton process	[84]
8	Methyl orange (dye)	US/EC-UV	Quartz photoreactor immersed in ultrasonic cleaning bath, temperature 25 °C, 11 W UV lamps with central wavelength of 253.7 nm, TiO_2 nanotube working electrode, saturated calomel reference electrode, platinum counter electrode, TiO_2 nanotube array grown by anodization of titanium sheets (15 mm × 7 mm × 0.5 mm) in hydrofluoric acid solution, anodization voltage 20 V, anodization time 20 min	Pseudo-first-order kinetics, decolorization rate were 0.0732 min^{-1} for US/EC/UV-catalysis process, 0.0523 min^{-1} for EC/UV-catalysis process, 0.0073 min^{-1} for US/UV-catalysis process and 0.0035 min^{-1} for UV-catalysis process, synergistic effect existed in the US, EC-assisted and photocatalytic process	[85]
9	1,3-Dinitrobenzene and 2,4-dinitrotoluene	US/EC-ozone	100 cm^3 thermostatted glass cell fitted with a gas-supply tube, titanium US horn radiator cathode, anode introduced through a side wall of the cell, anode and cathode compartments separated by MA-40 membranes, piezoceramic transducer of titanium horn waveguide with a working surface area of 5 cm^2, power intensity 5 W cm^{-2}, gas-discharge generator for ozone production from oxygen, oxygen flow rates 0.1–3 dm^{-3} h^{-1}, 50 mA, voltage 3 and 5.5 V, temperature 20–25 °C	Stable reaction of compound with ozone, US enhances the rate of EC reduction, application of US and ozonation to the EC reaction allows virtually complete destruction of the compounds in short times, US enhances EC process giving intermediates that are susceptible to ozone oxidation	[86]

occurred. The efficiency of this combined process is significantly much higher than the reference degradation methods and the time required for full degradation is considerably shorter maintaining high performance up to concentrations which are higher than reference methods. 2 mM Fe^{2+} ions was obtained as optimum concentration and again it is reported to be lower than its reference techniques [22]. In the same year, Oturan et al., studied US/EC–Fenton process as a novel hybrid technique for the destruction of organic pollutants in water. Its high performance arises from the coupling between US irradiation and the in situ electrogeneration of Fenton's reagent. For EC–Fenton reaction, an undivided electrolytic cell with a Platinum anode and a three-dimensional carbon-felt cathode have been used. The application of constant current is considered to produce numerous hydroxyl radicals which is good. Notable synergy is reported to achieve at low and high frequency within a range of output power which is due to the action of sonication in the US/EC–Fenton process. The degradation of all the compounds was observed to follow pseudo-first order kinetics. Among the pollutants studied, no improvement was observed for the degradation of the dye azobenzene (AB) only, demonstrating the importance of organic structure. In terms of power applied, lower power with 20 W was found to be better. The main reasons for the improved performance have been summarized as due to the cavitational pyrolysis, additional production of hydroxyl radicals by bubble collapse and improved mass transfer rate of Fe^{3+} and O_2 generating more EC–Fenton's reagent (Fe^{2+} + H_2O_2) [80]. Babuponnusami et al. studied a step ahead by comparing the performance of Fenton, EC–Fenton, US/EC–Fenton and UV/EC–Fenton treatment methods on the degradation of phenol. The degradation trend followed: UV/EC–Fenton > US/EC–Fenton > EC–Fenton > Fenton. Only UV/EC–Fenton and US/EC–Fenton achieved 100% degradation. Besides, UV/EC–Fenton process showed complete removal and 64.19% of mineralization within 30 min, whereas in the case of US/EC–Fenton process, mineralization observed at optimum conditions was 67.93%. The corresponding rate constant values for US/EC–Fenton and UV/EC–Fenton were 0.0683 and 0.0934 min^{-1}, respectively [81]. On a different note, Li et al. evaluated the effect of low frequency US irradiation on the US/EC–Fenton oxidation process in an acid aqueous medium. H_2O_2 production rate increases dramatically and the maximum concentration was obtained within a short period of timed. Hence, a considerable effect was contributed on pseudo-first-order degradation of cationic red X-GRL in the US/EC–Fenton process. Furthermore, the degradation rate was increased with increasing power and both TOC removal efficiency and mineralization current efficiency were significantly enhanced in comparison to basic EC–Fenton process. Therefore, for colored wastewater, US/EC–Fenton process is quite promising [82]. Another work based on US/EC–Fenton process is conducted by Martinez et al. using azure B as model pollutant. The frequency used was 23 kHz and H_2O_2 was generated electrochemically at reticulated vitreous carbon electrode. The degradation rate was studied under the effect of pH of the solution and initial concentration of Fe^{2+}. It followed apparent first-order kinetics in all the degradation processes and the highest was obtained at pH between 2.6 and 3. The degradation trend decreased in the following order: US/EC–Fenton > Fenton > US. The enhancement of degradation using US/EC–Fenton was ~10-fold more than US alone and ~2-fold more than Fenton alone. The COD removal using Fenton alone and US/EC–Fenton were ~68% and ~85%, respectively with removal of over 90% in both the processes [83]. Sahinkaya et al. also studied COD and C.I. Reactive Black 5 color removal from synthetic textile wastewater by US assisted EC–Fenton oxidation process. Optimal conditions were found as the initial pH of 3, DC current of 0.25 A, H_2O_2 dosage of 800 mg/L and electrode distance of 2.5 cm for both EC–Fenton and US/EC–Fenton processes. The assistance of US on EC–Fenton negligibly improved in terms of COD and color removals in comparison to EC–Fenton process [84].

Zhang et al. has claimed for the first time the use of hybrid processes involving both EC-assisted and US assisted ways to enhance the photocatalytic efficiency calling the whole process as sonophotoelectrocatalysis. In their work, the highly ordered TiO_2 nanotube array was fabricated on the pure Ti sheet with anodization technology in hydrofluoric acid solution, and was used not only as photocatalyst in sonophotocatalytic and photocatalytic processes but also as photoelectrode in photoelectrocatalytic and sonophotoelectrocatalytic processes. The system was used to treat azo dye, methyl orange (MeO). Particular attention was paid to the synergistic effect existing in the hybrid processes of US, EC and photocatalytic oxidation and the effect of operating conditions on US/EC-photocatalytic decolorization. In the process, current response in dark was insignificant even at a potential of up to 1.4 V, which meant that no EC oxidation occurred. Under illumination, a significant increase in the photocurrent was observed throughout the potential window. Moreover, the photocurrent was potential dependent, it increased as the applied potential increased, and reached the saturated state at a positive potential of 0.6 V. The photocurrent in MeO solution was higher than that in supporting electrolyte, which may be due to MeO providing a much more facile pathway for the transfer of holes across the film/electrolyte interface, resulting in the higher photocurrent density. The significant increase in photocurrent density with US irradiation may be due to the agitation effect induced by US cavitation. 0.6 V was applied in processes where EC is involved and vigorous agitation was used all the processes. The degradation trend of the processes within 60 min followed UV-catalysis < US/UV-catalysis < UV/EC-catalysis < US/EC/UV-catalysis. The US/UV-catalytic degradation of MeO was proven to enhance the photocatalytic efficiency because of the presence of ultrasound irradiation. In the presence of US, water hydrolysis under the extreme pressure and temperature conditions created by the implosion of cavitation bubbles produces hydroxyl radicals. The ·OH radicals could oxidize organic matters in aqueous solutions, and enhance the degradation efficiency of the MeO. In the case of EC-photocatalytic process, the recombination of photogenerated hole/electron pairs was suppressed by the external electric field, and thus the life of the holes and electrons got longer. Hence from the combined reasons given above, it is fair for the US/EC/UV-catalytic process to be the fastest among them. The pseudo-first-order kinetic rate of US/EC/UV-catalysis with 0.0732 min^{-1} was more than 20 times higher than that of photocatalytic process with 0.0035 min^{-1}. Hence, an obvious synergistic effect can be concluded to exist among the EC, US, and photocatalytic process [85].

As for the integration of ozone system, the mechanism described below [86] is based on the fact that molecular O_3 can be reduced to one of the most active oxidizing agents O_3^- ion (electron donor, D), at cathode (as given in Eq. (7) below):

$$O_3 + e^-(D) \rightarrow O_3^-(+D^+) \quad (7)$$

The O_3^- ion is a stronger oxidant than molecular ozone and in acid media rapidly undergoes reaction with the formation of the $O^{-\cdot}$ anion–radical and oxygen:

$$O_3^- \rightarrow O^{-\cdot} + {}^1O_2 \quad (8)$$

Alternatively, it can interact with water, giving oxygen, hydroxyl ion and radical ·OH proving that cathodic reduction of ozone yields highly active oxidizing agents as in Eq. (9):

$$O_3^- + H_2O \rightarrow HO^{\cdot} + {}^1O_2 + HO^- \quad (9)$$

On the other hand, the use of US enhances the rate of EC reduction but the overall rate of reaction is still slow. The main cause for the irradiation of US on an EC system is to accelerate the reactions at the electrode which is successfully proved. US can also enhance oxidation by ozone. Oxidation of organic compounds by ozone or a combination of ozone with hydrogen peroxide in a US field is enhanced in a low electric field. Besides, it increases the rate of diffusion processes and, as a consequence, speeding-up of the process of EC reduction of ozone.

So far, to our best of knowledge, for US/EC-ozone also, only Abramov et al. has reported for the degradation of 1,3-dinitrobenzene (DNT) and 2,4-dinitrotoluene (DNB). The cathodic reduction in an acid medium occurs in three stages with final product of diamine in 30 min. In the absence of US, it is reported that relatively little reaction took place and over the initial 10 min period the system operated at a current efficiency of 15%; whereas, under US treatment the current efficiency during the first 10 min increased to 55–57%. The observed increase in current efficiency compared with the corresponding unsonicated reactions can be attributed to the speeding-up of mass transfer processes in the aqueous medium. The rate of electrochemical reactions is usually limited by diffusion of reactants and products to and from the electrode surfaces. It is known that US irradiation leads to an increase in the effective diffusion of both ions and molecules in a liquid so that, in an US field, an acceleration of redox processes is observed.

It is also further reported that, if the reaction is carried out under oxygen rather than air during EC, the rate of the consumption of DNT and DNB is relatively insensitive to the US field after the initial stages of the reaction. The reaction is initially faster under US but reaches the same level of reaction after a short time and the availability of the oxidant is not a limiting factor in these reactions. In the report, it has been assumed that the primary reaction occurring at the cathode is due to the reduction of oxygen rather than the dinitrocompounds. Under the US irradiation, the acceleration of reduction of both oxygen and dinitrocompounds occur at the cathode, nevertheless, its rate decreases with a decrease in the relative concentration of DNT and DNB. Thus, US treatment does not significantly change the rate of DNT and DNB reduction when oxygen is bubbled through the solution. On the other side, in the absence of an electric field, the destruction of DNT and DNB by ozone is slow. The rate is faster under US but the level of conversion without the use of EC treatment does not exceed 15–20% for 30 min of treatment. Thus, DNT and DNB are fairly stable to oxidation destruction by ozone, even with the use of additional US treatment. However, carrying out simultaneous EC and ozone treatment under US leads to a dramatic increase in the rate of DNT and DNB consumption. Almost complete destruction can be achieved with this combined treatment. This large enhancement of nitroaromatic destruction can also be attributed to an increase in the rate of diffusion processes and, as a consequence, speeding-up of the process of EC reduction of ozone. During the passage of ozone, its reduction at the cathode rather than that of the nitrocompounds most probably occurs. This is suggested by the decrease in the rate of consumption (a combination of the processes of oxidation by ozone products and electrochemical reduction) of the reactants during the passage of ozone in comparison with simple electrochemical reduction. Despite the probable formation of more reactive O_3^- ions at the cathode, the oxidation destruction of DNT and DNB occurs very slowly without the use of US treatment. This could be due to the high activity of O_3^- anions which are unstable in acidic or neutral media and very rapidly consumed. However, under US irradiation along with ozone, a significant increase in the rate of consumption of DNT and DNB is observed with 100% degradation of the original product within 30 min. The contribution of US can be seen from the point of local heating of the medium during the cavitation collapse and dramatically enhanced mixing, diffusion and mass transfer by it. As the horn can be regarded as cathode the relative concentration of O_3^- near its surface can be significantly higher than that without US treatment, accelerating the oxidation of DNT and DNB on it. Hence, only under the combined application of US and EC with ozone, significant degradation rate of DNT and DNB is obtained [86].

7. Case study on pollutant degradation using sonoelectrochemical technology

7.1. Dyes

The conventional methods for the degradation of dyes include activated carbon, filtration, coagulation, etc. However, these methods have their own limitations. Textile industry effluents contain a variety of complex compounds with wide varieties of concentrations and types. However, by applying US/EC-oxidation, Lorimer et al. showed a successful and efficient degradation of dye effluent. The process involves determining the rate of decolorization by generating hypochlorite ion in situ, which is a powerful oxidant. By designing a sonoelectrochemical system, his group has proved a successful decolorization of acidic Sandolan Yellow in aqueous saline solution using platinum element. However, when US alone was irradiated with 20 and 40 kHz, the color of a solution of the acidic dye, Sandolan Yellow, was unaffected. It was also found to be resistant to 0.5 mol dm^{-3} of hydrogen peroxide. However, the addition of sodium hypochlorite solution (2.5×10^{-4} mol dm^{-3}) was able to effectively decolorize a solution of Sandolan Yellow (1×10^{-4} mol dm^{-3}) [18].

Rivera et al. found the combination of conventional physicochemical techniques as an effective option to apply to wastewater treatment which resulted in application of hybrid sonoelectrochemistry technique to increase the efficiency of textile wastewater remediation. Results have demonstrated the superiority of the sonoelectrochemical process over each treatment alone. When US alone was irradiated for 120 min, only 1% of dye was degraded indicating that US alone is not enough to mineralize complex compounds like textile dyes. When, sonoelectrochemical degradation was operated in a flow type system at the optimized conditions (0.0025 mol L^{-1} of Na_2SO_4) with a total reflux of 4.5 mL min^{-1}, significant superiority of the hybrid technique over the electrochemical alone was again detected. After 2 h of treatment of Lissamine Green B, a significant degradation of around four times that obtained by the electrochemical treatment was achieved. During the sonoelectrochemical treatment, intense agitation of the liquid and continuous degassing on the electrodes surfaces was detected. Using combined US/EC also, the decolorisation pattern is different according to the dye type due to variation in chemical structure and substituent. Thus, di-azo dyes such as Reactive Black 5 and Acid Black 24 were degraded less efficiently than the mono-azo or diphenylnaphthylmethane dyes which may be due to the type of chromophore group present. Mono-azo or diphenylnaphthylmethane are structural groups more easily breakable than di-azo groups. Besides, in the presence of an inert electrolyte, Na_2SO_4, the kinetic coefficients depend nonlinearly on the Na_2SO_4 concentration. Usually an inert salt increases the electric current densities in a solution leading to increased reaction rate with increased electrolyte. However, in this case, an optimum concentration of around 0.0025 mol L^{-1} of Na_2SO_4 was obtained [87].

On the other hand, Ai et al. developed a novel US-assisted EC system for effective decolorization of azo dyes in aqueous solution. Unlike others, the sonication was administered in pulses with a 50% duty cycle. Fresh air of 5 L min^{-1} was pumped from below

the cathode and to establish an adsorption/desorption equilibrium between the solution and the electrode, it was kept in the dark for half an hour. This novel set up gave a significant synergistic effect [88].

Siddique et al. studied the reaction kinetics and reaction mechanism for the decomposition of RB 19 dye by US assisted EC process. 90% of the dye was found to be degraded using the combined method within 120 min, whereas, when individual processes of US and EC were applied, only 13% and 52% were degraded respectively. Hence, a significant synergy was obtained for this study too showing the efficacy [42]. Giray et al. took one step ahead by combining Fenton reaction with US/EC process for the oxidative decolorisation of real textile wastewater. The US/EC–Fenton process was performed by indirect sonication in an ultrasonic water bath, which was operated at a fixed 35 kHz frequency and 80 W powers. The decolorisation efficiency for the Fenton process increased from 95% to 98.12% for Pt–Co dye [89]. Table 3 shows the list of dye degraded by US/EC process till date.

However, to our best knowledge, none of the reported cases of dye degradations using sonoelectro-oxidation has given clear explanation on the type of mechanism from which we can conclude it to be direct or indirect reaction.

7.2. Pesticides

Few cases for the successful degradation of pesticides using US/EC-oxidation have also been reported. Yasman et al. reported the detoxification of the common herbicide 2,4-dichlorophenoxyacetic acid (2,4-D) and its derivative 2,4-dichlorophenol (2,4-DCP) using a combination of US waves and EC oxidation at nickel electrodes. However, in this case Fenton process was also incorporated [22]. Pilot scale US/EC–Fenton process was more efficient than individual US and EC processes as well as combined US/EC process. The system consumes less time, power and it can be readily engineered. Likewise, Esclapez et al. tried to scale up the US/EC system by using an organic compound, TCAA. By employing EC system alone, the degradation yielded a poor performance. However, when a specifically designed reactor incorporated with US was used during the scale-up, better results with fractional conversion 97%, degradation efficiency 26%, selectivity 0.92 and current efficiency 8% were obtained. They also reported that the EC degradation of TCAA and its main by-products (DCA and MCAA) is enhanced by high frequency US, not only by improving the progressive C–Cl bond cleavage mechanisms, but also by enhancing the dissociative adsorption/incineration paths that occurs on both the cathode and the anode [40].

In another case, the degradation and mineralization of diuron (N-(3,4-dichlorophenyl)-N,N-dimethyl-urea) was analyzed for the first time using US/EC. A synergistic of 43% was achieved at a condition of 60 mA cm^{-2}, 20 kHz, 10 °C, pH 12 and 8 h of experimental running [90]. Table 4 shows the list of pesticides degraded by US/EC till date.

7.3. Pharmaceuticals

The application of US/EC in wastewater contaminated with pharmaceutical pollutants is still under development, though it is potentially a promising process. There are many peer reviewed papers on the degradation of pharmaceutical products using the individual methods, i.e., EC and US. However, no publications have been found except the recent most work done in our laboratory using the combined method. The degradation of Ibuprofen was investigated using US/EC method, and the kinetic rate constants were calculated. The system parameters studied were types of electrolyte, its concentration, frequency, applied voltage, ultrasonic

Table 3
List of dye degraded by US/EC process.

	Pollutant	Equipment/Experimental conditions	Important findings	Refs.
1	Sandolan Yellow	500 cm^3 flasks placed in a water bath (60 °C) for 3 h, platinum and carbon working electrodes, supporting electrolyte NaCl, current 100 mA, frequency 40 kHz, power 22 W.	Optimum power 22 W, chlorine liberated at anode, hydroxide ion at cathode, in situ generation of hypochlorite ion, no decolorization with US alone, platinum electrode better than carbon	[18]
2	Reactive Blue dye	Undivided electrolytic cell made up of Perspex sheet, electrodes positioned vertically and parallel to each other, interelectrode gap 2.5 cm, lead oxide anode (14–15 cm^2), stainless mesh steel cathode, Digital Ultrasonic Bath, pH range 3–9, US frequencies 20–80 kHz, pH maintained using1 M NaOH or 1 M HCl	e 90% color removal and a maximum of 56% TOC removal for 50 mg L^{-1} dye concentration of un-hydrolyzed achieved at US frequency of 80 kHz, pH of 8 after 120 min	[42]
3	Acid black 24 Lissamine Green B Methyl Orange Reactive Black 5 Trupocor Red	Cylindrical glass cell, graphite electrodes (effective area 7 cm^2), electrode gap 4 cm, probe type US generator, frequency at 20 kHz with cycle 10%, power 60%, supporting electrolyte Na_2SO_4	Combined US/EC superior than individual system, color removal considerably faster than the decrease in COD which is attributed to the ease of chromophore destruction, Lissamine Green B decolorization efficiency is 95% compared to 60% of COD removal after 1 h treatment, first-order kinetic, decolourisation rate of the diazo dyes such as Reactive Black 5 and Acid Black 24 lower than mono-azo or diphenylnaphthylmethane dyes, optimized conditions for flow system are 0.0025 mol L^{-1} Na_2SO_4 and total reflux 4.5 mL min^{-1}, decolourisation percentage obtained after 2 h of Lissamine Green B by US/EC is around four times that obtained by the EC	[87]
4	Rhodamine B	Cylindrical water-jacketed glass reactor (200 mL), titanium probe transducer with 1 cm tip diameter, 2 cm of tip put into the liquid phase, pulse sonication with a 50% duty cycle, reactor immersed into a water bath, constant temperature 25 °C, potentiostat mode, initial pH adjusted with 0.10 M H_2SO_4 or 0.10 M NaOH, 5 L min^{-1} of fresh air fed, Pt sheet anode(area 2.0 cm^2), ACF working cathode (area 3.0 cm^2), supporting electrolyte Na_2SO_4, frequency 20–50 kHz, power 400 W.	Rhodamine B decolorized completely using US/EC system, 91.4% degradation within 6 min which is much higher than that of US (0.4%) or EC (24.5%) process, high synergy	[88]
5	Textile dye	Batch, 1000 mL flask in US bath, wastewater volume 500 mL, iron plates as anode and cathode (dimensions 40 mm × 90 mm × 10 mm), electrode gap 1 cm, pH adjustment by 0.5 M H_2SO_4 and 0.5 M NaOH, pH 2.0–3.5, H_2O_2 concentrations 150, 160, 170, 180 μL/L and current 0.01, 0.05, 0.1, 0.15, 0.25 A, frequency 35 kHz, power 80 W	Optimum conditions are 150 μL/L H_2O_2, 0.15 A current density and pH 2.7, dye removing efficiency are 97.03% for Pt-Co, 96.40% for 436 nm, 97.95% for 525 nm, 98.15% for 620 nm	[89]

Table 4
List of pesticides degraded by US/EC process.

	Pollutant	Equipment/experimental conditions	Important findings	Refs.
1	2,4-Dichlorophenoxyacetic acid (2,4-D) 2,4-Dichlorophenol (2,4-DCP)	Glass cylinder vessel reactor (internal diameter 25 mm), effective sample volume 10 mL, solution temperature 25 ± 1 °C, double jacket cooling array circulated, horn type sonication via titanium alloy tip (13 mm in diameter) dipped in from the top of the reactor, average output electric power 75 W, frequency 20 kHz, nickle foil cathode and anode (0.125 mm thin) with cylindrical segments (11 mm radius, 20 mm height), placed around a horn (11 mm radius), Na_2SO_4 (0.5 g/l) supporting electrolyte, galvanostatic mode, current intensities not exceeding 100 mA	50% oxidation of 2,4-D solution (300 ppm, 1.2 mM) in just 60 s, full degradation in 600 s, US/EC-Fenton degradation efficiency higher and takes considerably shorter degradation duration, optimum concentration of Fe^{2+} ions about 2 mM	[22]
2	Chloroacetic acid	Laboratory glass US reactor (adapted for US/EC also) used for bulk electrolysis in batch mode, galvanostat (120 mA_13.4 V maxima power), catholyte volume 200 mL, for divided mode, a Nafion 450 cationic membrane to separate catholyte and anolyte chambers, with anolyte volume 200 mL, for non-optimized flow-US/EC system used for the scale-up of the process, polypropylene reactor designed for divided and undivided configuration, catholyte and anolyte volume 2000 and 1000 mL, respectively, titanium disk with d = 4 mm, 0.126 cm^2 and spiral wound platinum wire cathode for voltammetric experiments, for bulk electrolyses, mesh-plate of Ti with 2 cm^2 of active area in each electrode face in the batch cell and 20.0 cm^2 in the flow cell used as cathodic material and platinized titanium (Pt/Ti) mesh with 20 cm^2 as anodic material in both scales, reference electrode is an Ag/AgCl/KCl (3 M), supporting electrolyte Na_2SO_4 purged with argon to avoid oxygen entrance, frequency 358,850,863 kHz, power: 0.039, 0.047, 0.054 W	US alone gave poor performance compared to US/EC, batch scale US/EC analyses with horn-transducer 24 kHz positioned at about 3 cm from the electrode surface achieved little degradation, but specifically designed sonoelectrochemical reactor (not optimized) during the scale-up, provided better results (fractional conversion 97%, degradation efficiency 26%, selectivity 0.92 and current efficiency 8%) at lower ultrasonic intensities and volumetric flow	[40]
3	Diuron	Undivided cell of 0.25 L borax glass reaction vessel with thermal jacket, two rectangular BDD electrodes (area 11.4 cm^2), electrode gap 5 cm, titanium US horn (13 mm length) placed at 2.6 cm from the reactor bottom, 1.8 cm gap between the horn and each electrode, galvanostatic mode, constant current density of 60 mA cm^{-2}, batch mode, pH 2 and 12, temperatures between 10 °C and 40 °C, frequency 20 kHz, power 750 W	43% degradation at j = 60 mA cm^{-2}, US = 20 kHz, pH = 12, T = 10 °C and 8 h, alkaline pH favors the mineralization rate with total organic carbon degradation higher than 92% after 6 h, weak impact when temperature is between 10 °C and 40 °C	[90]

power and temperature. In addition to the above, the development of an efficient degradation system was examined considering energy consumption, energy efficiency, and synergistic effects of the applied methodologies. Experimental results show that, when alkaline electrolyte of NaOH was used, both EC and US contributed significantly, leading to more efficient degradation than using acidic low pH electrolyte. The results were achieved by applying constant electrical voltage of 30 V, high US frequency of 1000 kHz and power density of 100 W L^{-1} at 298 K in 1 h, proving that US/EC system employing NaOH as electrolyte for the degradation of IBP is worthwhile and feasible. Besides, synergistic effect was also achieved without using any electrolyte proving that the combined system can be employed without the need of any additional chemical [55]. Fig. 1 shows the schematic diagram showing the synergistic mechanism for the US/EC oxidation of Ibuprofen (IBP) from the same study.

Apart from degradation studies, many more works on different fields have also been done as an expanding work using this combined US/EC technique. Analysis on corrosion, batteries, photoelectrochemistry, bioelectrochemistry and sensors are a few more applications of importance using US/EC. However, the main scope of this present review study covers the importance of the application for environmental remediation. Hence, a more intensive literature study of its possible improvement techniques is done in the preceding sections, especially by exploring its practical engineering side.

7.4. Miscellaneous

The degradation of some organic pollutants, especially the refractory materials present in the wastewater is still cumbersome. Application of a single physical or chemical treatment in many cases is inadequate because of their complex structures. However, the synergistic production of highly reactive radicals by the combination of several advanced oxidation processes has been proved to be one of the promising treatment technologies for this kind of pollutants in recent years [91]. Among them again, US-enhanced EC oxidation (US–EC process) is one of the hybrid emerging technologies being studied by many researchers exploring its potential. Many researchers demonstrate on its synergistic enhancement [75] as an alternative to carry out the mineralization of bio-recalcitrant compounds.

In 1996, a different configuration of US/EC reactor was developed where the ultrasound emitter was simultaneously used as working electrode (sonotrode). By using it, the electro-reduction of organic solvents, namely benzaldehyde and benzoquinone under the exposure of ultrasound was investigated. The mass transport rate, rates of production of reduced organic compounds and current intensity were observed to be enhanced without changing the reaction mechanism [92]. In the same year, Trabelsi et al. evaluated the influence of low and high frequency US on mass transfer phenomena. His team determined the active zones in the reactor along with the study of phenol at a gold cylinder anode [4]. On the other hand, Leite et al. proposed an integrated process for the oxidation of 2,4-dihydroxybenzoic acid at platinum electrode by combining low and high frequency ultrasounds with an electrochemical system [21]. Lindermeir et al., giving more interest on technical domain, employed a unique configuration for the oxidation of p-methoxytoluene. In an undivided cell, a graphite anode was mounted upwards from the bottom of the reactor and used a platinum wire spiral as counter electrode. The anodic oxidation of was investigated using an ultrasound probe with a titanium tip positioned "face-on" to the anode [93].

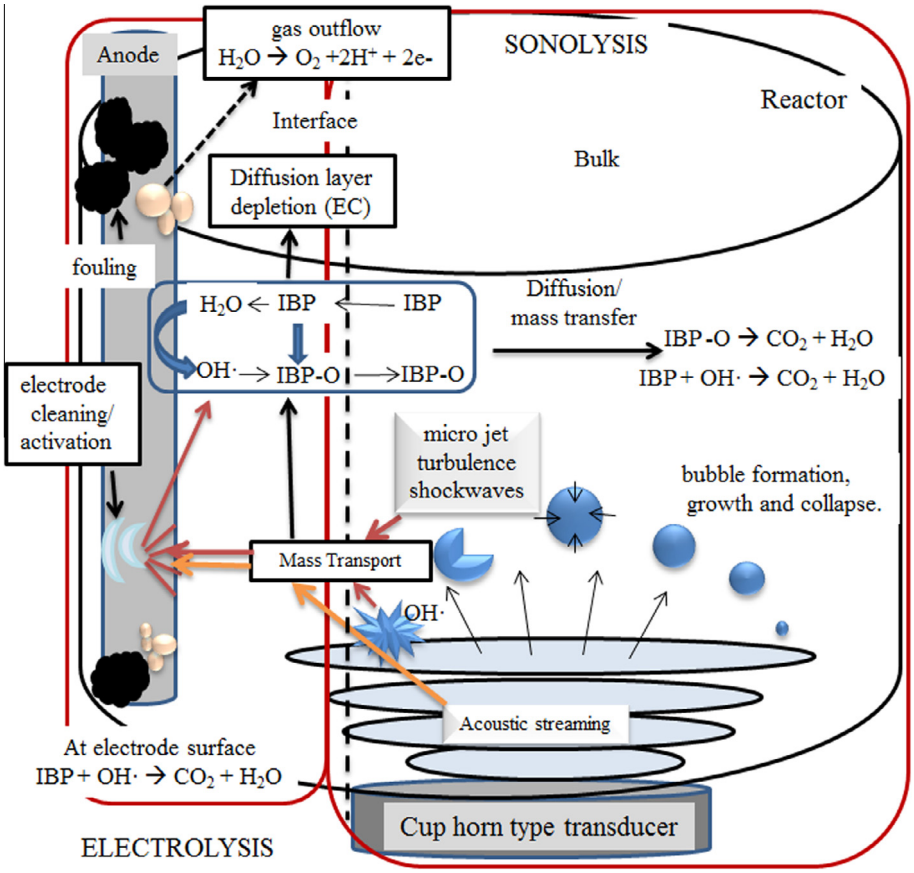

Fig. 1. Schematic diagram showing the synergistic mechanism for the sonoelectrochemical oxidation of Ibuprofen (IBP) [65].

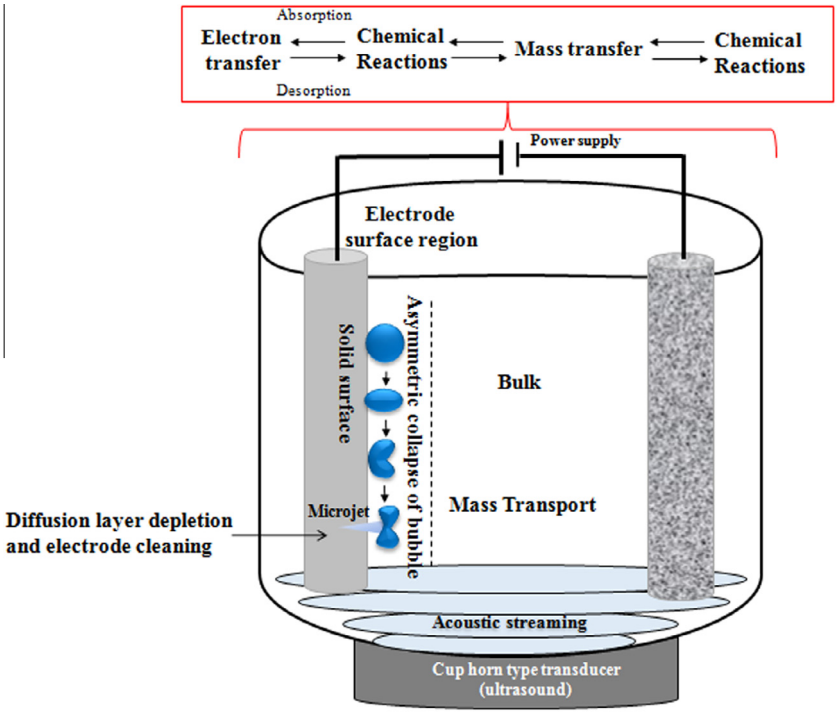

Fig. 2. Schematic diagram showing the asymmetric collapse of bubble, microjet formation near the electrode surface and induced electron-mass transfer.

Other researchers also conducted the experiment of organic degradation using different types of electrodes. Zhao et al. claimed that the integration of US in EC can lead to the amplification of phenol degradation rate. The research was conducted using different electrodes. With BDD, the degradation rate and current efficiency were increased by 301% and 100%, respectively; while using Pt, the increment were 51% and 49%, respectively when facilitated with US. The peak current density of the combined process also showed an enhancement in different degree. For BDD anode, it increases to 8.1 mA cm^{-2}, by 108%, and to 6.4 mA cm^{-2}, by 25% at Pt anode, proving that US can enhance the direct oxidation of phenol [38]. They also studied for the organic compound phthalic acid in the preceding year [94].

Sáez et al., studied the US/EC degradation of perchloroethylene at 20 kHz using controlled current in batch mode. A fractional conversion of 100% and a degradation efficiency of around 55% were obtained. The main volatile compounds produced in the EC and US treatment, trichloroethylene and dichloroethylene, are not only totally degraded, but they were removed at shorter time than in the US or EC treatments [95]. On the other hand, the influence of the presence of a background electrolyte on the efficiency of the US/EC degradation of perchloroethylene (PCE) in aqueous solutions has also been analyzed using batch mode. 100% degradation efficiency was achieved at a higher ultrasonic power intensity level of 7.64 W cm^{-2} [96]. Ren et al., made a different approach for treating phenol. The anode was a stainless steel spherical net (diameter: 43 mm; surface area: 4950 mm^2; mesh size: 0.16 mm^2, wire diameter: 0.15 mm), and the cathode was stainless steel ring (diameter: 50 mm, thick: 2.8 mm). The configuration coupled with a high-frequency of 850 kHz gave 60% synergetic effect [72]. Table 5 shows the list of organic pollutants degraded using US/EC till date.

8. Optimization of degradation methods using US/EC: emphasis on reactor design and operating parameters

By simulating the performance of the US/EC system with reference to different geometric aspects, configuration and operating conditions, the optimum design of US/EC reactor can be determined. While designing the optimized system several important factors contributing toward adaptability, energy efficiency, automation and environmental friendliness should be taken into account. Few basic parameters which directly or indirectly affect the degradation mechanism of the system are described below:

8.1. Ultrasound emitter

In the ultrasonic bath type emitter, the cell is electrically separated and the sound waves penetrate a glass wall before entering the EC reactor [97]. For this type of configuration, the intensity of bubble production and the formation of reactive radicals are considered to be reduced. The frequency is also fixed and in most cases ranges between 20 and 100 kHz. However, in the ultrasonic immersion horn probes, the horn can supply higher US intensities (10–1000 W cm^{-2}). The anatomic difference can be seen in Fig. 3. In this type, the radiation directly applied to the EC system can be controlled by the amplitude of the tip vibration [15]. Its average intensity at the tip can be calculated using Eq. (4) [98]:

$$p_\alpha \approx \sin\frac{\pi}{\lambda}\left[(x^2+r^2)^{\frac{1}{2}}-x\right] \tag{10}$$

where x is the distance from the horn, r the radius of the horn tip and λ is the wavelength. The intensity is expected to drop by 5% of its initial value when the distance is approximately similar to the horn diameter and further drops by $\frac{1}{x^2}$ approximately. Around

Table 5
List of miscellaneous organic pollutants degraded by US/EC process.

	Pollutant	Equipment/Experimental conditions	Important findings	Refs.
1	Benzalaldehyde Benzoquinone	Immersion horn system, piezoelectric ceramics transducer, frequency 20 KHz, three electrodes system with saturated sulfate reference electrode (+0.656 V vs. nhe), platinum grid counter electrode, titanium horn working electrode, NaCl (2.5 M) as supporting electrolyte	No switching of reduction mechanisms but dramatic changes in the EC behaviors of electroactive species, modifications of the *I/E* curves under cyclic voltammetric conditions and *I/t* curves under constant applied potential seem to be due to perturbation of the electrode-solution interface by collapses of the cavitation bubbles at the near vicinity of the sonoelectrode surface and an increase of the mass transfer by US stirring, reduction rates notably increased except when the solvent decomposes under US irradiation	[82]
2	Phenol	200 cm^3 glass cylindrical reactor (internal diameter 7 cm), gas bubbled, constant temperature 27 ± 2 °C by water–ethylene glycol mixture circulation, output electric power 50 W, power dissipated in the medium 20 W, for 500 kHz: submersible stainless steel piezoelectric transducer with 12 cm diameter fixed at reactor's bottom, for 20 kHz: an immersible horn with a titanium alloy rod (13 mm diameter) dipped in the liquid at the top of the tank, cylindrical nickel foam cathode (Ø3 6.4 cm, height 4 cm, specific area 4000 m^2 m^{-3}), cylindrical anode (Ø0 5.4 cm and high 4 cm) constituted of platinized titanium grid of expanded metal (mesh 8 60 60 and area about 147 cm^2), current intensity 1 A (current density = 68 A/m^2)	At 20 kHz sonication, phenol oxidation is 75% within 10 min with intermediate quinone formation, at 500 kHz, 95% degradation achieved with acetic and chloroacrylic acids as final products, mass transfer under high frequency US enhanced by 70-fold and 120-fold enhancement under low frequency, at 540 kHz, total degradation of phenol within 20 min with no toxic intermediate production	[4]
3	2,4-Dihydroxybenzoic acid	500 cm^3 cylindrical glass vessel reactor, thermostated by circulating a water–ethylene glycol mixture in the reactor jacket, piezoelectric transducer for 500 kHz, placed at the reactor's bottom, 20 kHz frequency produced by directly dipped horn, expanded platinized titanium grids electrodes, cylindrical electrodes for high-frequency, disks for low-frequency, total area of cylindrical anode and cathode 138 and 172 cm^2, respectively, total area of disk anode and cathode 52 × 2 cm^2, saturated calomel reference electrode, temperature 30 ± 3 °C, supporting Na_2SO_4 (0:1 M), pH 2, magnetically stirred when disk electrodes were used, mechanically stirred in the case of cylindrical electrodes. For linear sweep voltammetry with 500 kHz US,	At high frequency, hydroxyl radicals generated, at low frequency, accelerated mass transfer rates of the electroactive species from the bulk solution to the electrode surface as well as adsorption–desorption mechanisms. At low frequency, 47% TOC decrease with current 1:5 A h, at high frequency only 32% after passing 3:5 A h, 2,3,4- and 2,4,5-trihydroxybenzoic acids (THBA), maleic acid, glyoxylic acid and oxalic acid as by products, at low frequency, fewer intermediate aromatic compounds formed and faradaic yield increased with more efficient energy but the overall energy consumption remains high (~200 kW kg^{-1})	[21]

Table 5 (*continued*)

	Pollutant	Equipment/Experimental conditions	Important findings	Refs.
		platinum rotating disc working electrode with 3 × 14 mm^2 exposed surface, platinated titanium counter electrode, saturated calomel reference electrode, without US, 2000 rpm rotation speed, for linear sweep voltammetry with 20 kHz, platinum wire working electrode with 1 mm diameter and 2 mm^2 exposed surface, without US magnetically stirred (500 rpm), multifrequency piezoelectric transducer placed at reactor's bottom		
4	Toluenes	Undivided cylindrical cell (20 mm diameter), graphite anode, platinum wire spiral counter electrode, reference electrode positioned near working electrode to minimize ohmic drop, can operate in batch or closed circle mode, US probe with a titanium tip positioned "face-on" the anode, distance between the immersion horn and working electrode between 0 and 50 mm, US generated by HF transducer and stepped booster horn, frequency 20 kHz, power 70 W	Distances below 10 mm diminishes the increase in current due to the operation in bubble shield sound source, small gaps between the stepped horn and the graphite electrode favor poorer current densities because of the higher gas volume fraction, highest increase in current density results for distances between 10 and 20 mm, for larger gaps the effect becomes less distinctive	[83]
5	Phenol	Cylindrical single-compartment cell with jacketed cooler, BDD or Pt anode with 24 cm^2 immersed area, titanium foil with same area as cathode, interelectrode gap 1 cm, current density 20 mA cm^2, pH 3.0 adjusted with 0.2 M H_2SO_4, 200 cm^3 phenol sample volume, 10 °C temperature, solution volume 200 cm^3, frequency 33 kHz, 50 W	With US, for BDD, increased degradation rate and current efficiency are 301% and 100%, respectively, for Pt 51% and 49%, respectively, increased diffusion coefficient for BDD and Pt are 375% and 42%, respectively, US effect on BDD much greater than for Pt, without US large adsorption phenol on both electrodes, with US, the adsorption amount decreased by 79% and 56% on BDD and Pt electrodes, respectively, renewal and activation effect of US on the surface of BDD more obvious than Pt, enhancement for EC by US on BDD is 108% and for Pt is only 25%, degradation of Ph on BDD easier than Pt, lower amount of intermediates produced at BDD than Pt	[39]
6	Phenol (Ph), Phthalic acid (PA)	Cylindrical single-compartment cell, BDD anode (24 cm^2 immersed area, ~1 μm thickness), titanium foil with the same area as cathode, electrode gap 1 cm, current density 20 mA cm^{-2}. pH 3.0 using 2 M H_2SO_4, 200 cm^3 solution volume, frequency 33 kHz, power 50 W, temperature 10 °C	74% and 69% EC oxidation energy consumption (AE) for Ph and PA, respectively reduced by US, mass transport coefficients of Ph and PA both reached 2.0×10^{-5} m s^{-1} in US-EC process, from 5.4×10^{-6} and 6.7×10^{-6} m s^{-1} in EC, increasing by 270% and 199%, respectively, reaction amount of Ph decreased by 79% with US, from 6.49×10^{-10} to 1.39×10^{-10} mol cm^{-2}. For PA, the reaction amount decreased from 1.25×10^{-11} to 3.11×10^{-12} mol cm^{-2} with US, oxidation peak current increased by 32% for Ph, for PA, no direct oxidation happened in US-EC process	[84]
7	Perchloroethylene	Controlled-current or controlled-voltage galvanostat, current 120 mA, voltage 14.5 V, electrode-apart-transducer configuration, lead (4.5 cm × 2.5 cm × 0.3 cm) and lead dioxide (4 cm × 2.7 cm 0.6 cm) plates as cathode and anode, respectively, supporting electrolyte Na_2SO_4, frequency 20 kHz, power density 7.64 W cm^{-2}	Degradation more efficient with background electrolyte, 100% degradation efficiency achieved at higher US power level, current efficiency enhanced more in background-electrolyte-assisted US/EC treatment and a lower speciation in shorter times provided total degradation of the pollutant into non-chlorinated compounds	[86]
8	Perchloroethylene	Undivided reactor, frequency 20 kHz, power density 3.39 W cm^{-2}, electrode-apart-transducer configuration, lead (4.5 cm × 2.5 cm × 0.3 cm) and lead dioxide (4 cm × 2.7 cm × 0.6 cm) plates as cathodes and anodes, respectively, galvanostatic mode, 200 mL working volume, pH and conductivity changed from the initial values (6.0 and 7.3 mS cm^{-1}) to the final values (3.4 and 8.6 mS cm^{-1})	Improvement in US process with EC implementation, but lower EC treatment with 20 kHz US field, 100% fractional conversion and 55% degradation efficiency obtained independently for US power used, current efficiency also enhanced compared to EC treatment and higher speciation detected, volatile compounds produced in the EC and US treatments, trichloroethylene and dichloroethylene not degraded totally	[85]
9	Phenol	Double-walled cylindrical glass reactor, US transducer fixed at the bottom, continuous mode, frequency 850 kHz under an atmosphere of air, power 170 W, stainless steel spherical net anode (diameter 43 mm, surface area 4950 mm^2, mesh size 0.16 mm^2, wire diameter 0.15 mm), stainless steel ring cathode (diameter 50 mm, thick 2.8 mm), electrodes placed in the middle of the reactor so that transducer offers the highest acoustic energy and a high mass transfer is possible, supporting Na_2SO_4	60% synergetic effect for US/EC, high concentration of electrolyte and high electrical voltage favorable, nearly complete degradation with 4.26 g/L Na_2SO_4 and 30 V electrical voltages at 25 °C in 1 h, pseudo-first order kinetics	[73]

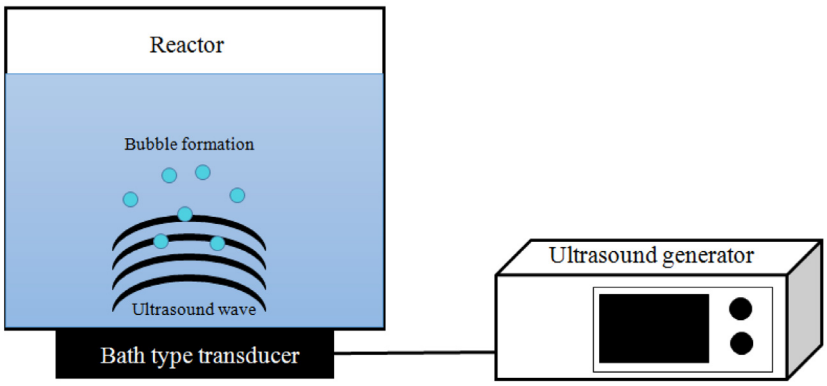

a. Ultrasonic bath type emitter.

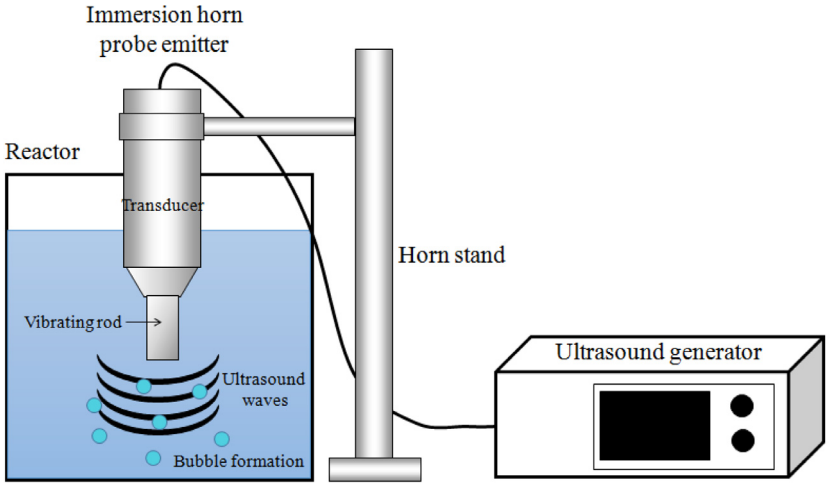

b. Ultrasonic horn type emitter.

Fig. 3. Types of ultrasound emitter.

the horn, the intensity is highest, providing suitable conditions to form cavitation. However, once the electrode is placed far enough from the horn tip, no cavitation takes place and hence the effect of microjet is also not visible. If an electrode surface is placed sufficiently close to the ultrasonic transducer, the periodic movement contributes to the signal current through the alternate increase or decrease of the transport of species to the electrode surface. Hence, the relative distance from the tip to the electrode is also used as a parameter for controlling the US radiation in the EC system [5].

In the case of bath type, the acoustic energy field is considered to be distributed evenly throughout the reactor, giving an equal impact on the electrodes. In the case of probe type, more intense energy can be dispatched to the electrodes, receiving effective physical phenomena of cleaning and more generation of reactive radical. However, the problem of tip erosion may be encountered, contaminating the system as well as reducing the efficiency of the horn [99].

Even though, the mechanical phenomena and the chemical aspects are largely altered by the types of ultrasonic emitter used, its comparative study in relation to US/EC-oxidation of pollutants has not been reported yet. Esclapez et al. tried studying the characterization of the non-optimized flow US/EC reactor using the acoustic field, but they considered only probe type. His team while introducing the concept of attenuation coefficients of 0.5, 1 and 5 m^{-1}, showed that it not only affects the magnitude of the average acoustic energy stored in the liquid, but also changes the form of the acoustic field inside the reactor. While applying 5 m^{-1}, a main pressure antinode and a secondary pressure antinode were obtained near the electrode. Since, cavitation on the surface of the electrode enhances the mass-transport as well as the degradation reaction; this particular result of acoustic simulation can be regarded as a valuable tool while designing an efficient US/EC reactor [40].

8.2. Ultrasound power

The sonochemical reaction rate is considered to increase proportionately with US power. The power intensity, which is a function of acoustic amplitude, is again proportional to the applied power density, P_A as given in Eq. (5):

$$I = \frac{P_A^2}{2\rho c} \tag{11}$$

where I is the sound intensity, ρ is the density of the medium, c is the velocity of sound in the medium, P_A is acoustic amplitude. Power intensity also controls various important parameters such as the cavitation bubble size, the bubble collapse time, the transient temperature, and the internal pressure in the cavitation bubble during the collapse. At high acoustic intensity (i.e., large P_A values in the equation given below), when the rarefaction cycle occurs, the cavitation bubbles bigger and collapse during a single compression

cycle. More can be known from the equation given in the Eq. (6) below:

$$R_m = \frac{4}{3\omega_a}(P_A - P_h)\left(\frac{2}{\rho P_A}\right)^{1/2}\left[1 + \frac{2}{3P_h}(P_A - P_h)\right]^{1/4} \quad (12)$$

where ω_a is the applied acoustic frequency and P_h is the external (hydrostatic) pressure. Besides, is proportional to the maximum bubble size, R_m also corresponds to the bubble collapse time, τ as seen in Eq. (7):

$$\tau = 0.915R_m\left(\frac{\rho}{P_m}\right)^{1/2}\left(1 + \frac{P_{vg}}{P_m}\right) \quad (13)$$

where $P_m = P_h + P_a$ is the pressure of the liquid and P_{vg} is the vapor pressure in the bubble. From the above equations, it can be concluded that there is an optimum power density at which maximum reaction rates can be obtained [100].

Moreover, in the combined US/EC process, it is one of the most important parameters as it relates directly to the current value of the redox process [101]. It is also directly related to the number of cavitation bubbles imploding at the electrode surface and the turbulence effect generated by the cavitational bubble which in turn increases the mixing intensity. The number of active cavitation bubbles increases with an increase in the acoustic power leading to an increase in the corresponding amount of OH^- radicals generated [102], which might be responsible for the observed enhancement in the degradation rates.

In a work done by Binota et al., the US/EC-oxidation rate constants of Ibuprofen was found to increase with increasing ultrasonic power density with the degradation trend of $100 > 80 > 60 > 40\ W\ L^{-1}$. The observed rate constants were in between 0.026 and $0.034\ min^{-1}$. In this study, until the power density of $100\ W\ L^{-1}$, no optimum value was found. However, keeping a check on the energy consumption trend and its efficiency as given in the same table, the application of lower power is recommended. In contrast, higher power gave the best efficiency from the viewpoint of degradation [65]. Table 6 shows the related study on dependence of degradation rate on power density. On the other hand, in a study done by Yang et al., an optimum power was obtained supporting the prediction done in the above equations. The TOC removal rate was reported to increase with increasing US power until it exceeded 250 W. After it, TOC removal rate gradually declines, suggesting that increasing the ultrasonic intensity did not always lead to an improvement in the TOC removal rate [100].

The existence of this optimum power can be further explained by the fact that the increased intensity can lead to increased number of cavity resulting into an increase total quantum of pressure energy liberated during the collapse of cavities, enhancing the corresponding degradation rate. However, further increased in power intensity simultaneously produces large numbers of gas bubbles in the solution leading to sound waves scattering, bubble cloud formation coalescence of the cavities. Hence, lesser energy is dissipated and attenuation of waves take place at very high intensity leading to deterioration of degradation after a certain point [103].

8.3. Frequency

For environmental pollutant degradation, high frequencies in the range of a few hundred to thousand kilohertz are generally employed in wastewater treatment. For applications like biotechnological, textile processing, solid–liquid extractions, etc. lower frequency are usually used [104]. Low US frequency is considered to enhance the mass transfer more than higher frequencies. Trabelsi et al. observed mass transfer enhancement of upto 70-fold at high frequency with maximum values measured in an intermediate zone between the axis and the reactor wall. In the case of low frequency, the mass transfer was higher by 120-fold, measured mainly on the reactor's axis. However, the degradation was higher at high frequency. At 20 kHz, the result of the US/EC destruction of phenol was 75% in 10 min. At 540 kHz, it was 95% conversion. Table 7 shows the dependence of degradation on frequency. Under high frequency sonication, the chemical effect of ultrasound may have dominated, either through bond cleavage of substrate or through water US (hydroxyl radical formation) [4]. In another case, when the sonication was used over 20–80 kHz range, the TOC removal rate was sharply increased till 45 kHz, and then the rate declined. This may be due to the enhancements in the cavitation-bubble pulsation and overcoming the mass-transfer effect at low frequency. However, the resonant radius of the cavitation bubble decreases with increasing frequency, weakening the cavitation intensity, leading to a decline in the TOC removal rate. At high frequencies, the rarefaction (and compression) cycles are very short. The time required for the rarefaction cycle is too short to permit a cavitation bubble to grow to a size, sufficient to cause optimal disruption of the liquid generating $OH^{\cdot}$ radicals [7]. In fact, their collapse energy became less. The collapse of this cavitation bubble takes place only when it reaches their resonant radius. This can be again supported by the relation below:

$$R_r \approx 3.28 f_r^{-1} \quad (14)$$

where R_r is the resonant bubble radius in millimeters and f_r is the resonance frequency in kilohertz. These two parameters are related inversely to each other [105]. The decrease in efficiency at higher frequency has been claimed due to higher acoustic power consumption too which may again correlate to the above description in power section [106]. Hence, the existence of optimum frequency is fair enough. On the other hand researches like Sivakumar, Tatake and Pandit have suggested for the intense cavitation production and higher value of pressure pulse generation using multiple frequency [107,108].

8.4. Liquid height

Significant enhancement in the reactions occurred, as liquid height is increased. Degradation activity is reported to increase

Table 6
Dependence of Ibuprofen (pharmaceutical compound) degradation on power density [65].

Power density (W/L)	Energy consumption (kWh)	Energy efficiency (mmol/kWh)	k (min^{-1})
40	0.033	0.0236	0.026
60	0.054	0.142	0.027
80	0.78	0.103	0.03
100	0.127	0.067	0.034

Experimental condition: sample volume: 1 L, temperature: 25 °C, Ibuprofen concentration: 2 ppm, frequency: 1000 kHz, working electrode: platinum plate, voltage: 30 V, k: pseudo first order kinetic constant.

Table 7
Dependence of Phenol degradation on frequency [4].

Time	Phenol conversion%	
	20 kHz	540 kHz
0	0	0
5	46	73.6
10	76	95
45	92.2	100
60	97	100

Experimental condition: sample volume: 0.2 L, temperature: 27 + 2 °C, power: 50 W, working electrode: gold cylinder, current density: $68\ A/m^2$.

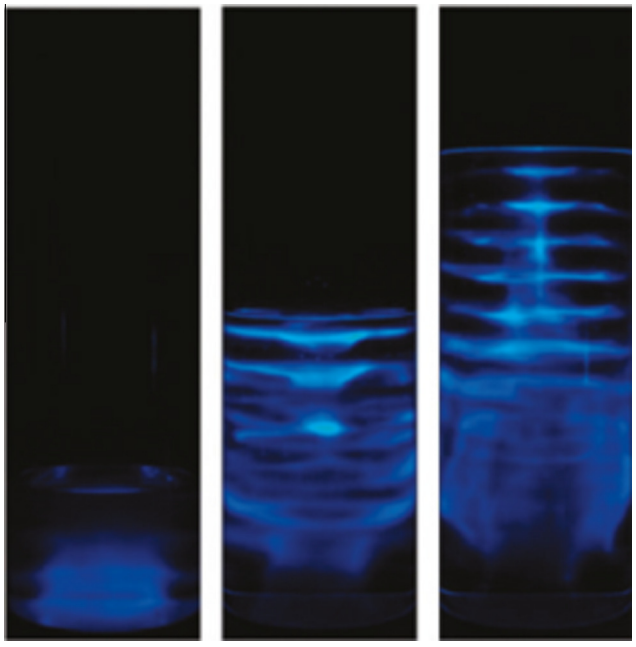

Fig. 4. Sonoreactor with different liquid heights at 36 kHz [109].

when liquid height/volume was increased and power density decreased exponentially, thereby affecting the production of hydroxyl radical enhancement. Son et al., has suggested for an optimized liquid height of water for the best efficiency. Fig. 4 clearly shows that with increased liquid height, the cavitation active zone is also expanded (blue waves seen in the figure), and hence the sonoactivity is also increased [109].

On the contrary, Renaudin et al. and Koima et al. studied liquid height at 25–75 mm and 20–70 mm respectively through US luminescence [110,111]. In both the studies, the US reactions were reduced with an increase in the liquid height; however the study was done at only a laboratory scale. In the case of Asakura et al., the study was made at industrial scale and they reported that the dependence of sonochemical efficiency (SE) on frequency and liquid height. It was shown that the peak of the SE value increases monotonically with the logarithm of the frequency, and the liquid height yielding the highest SE of approximately 15 times than normal condition. The empirical relationship between the SE value at the first peak and frequency is obtained using the following Eq. (9):

$$SE_{peak} = [1.5\log_{(f)} + 3.1] \times 10^{-10} \quad (15)$$

where SE_{peak} [mol J^{-1}] and f [kHz] denote the SE value at the first peak and the frequency, respectively [112]. Hence, according to this information, the optimization of large-sized sonochemical reactors for practical applications can be quantitatively analyzed and optimally designed.

Besides, it is also worth mentioning that, if the liquid height is specified for the scale-up of US reactors, the optimum frequency of US reactions can be determined. It can be seen from the relation given below which exhibited a satisfactory linear correlation and the following empirical relation was obtained using Eq. (16):

$$h_{peak} = \frac{23,400}{f} - 22.9 \quad (16)$$

where h_{peak} [mm] is the liquid height at the peak of the SE value and f is the frequency [113].

Kim et al. explained that a liquid height of less than h_{peak} give comparatively high ultrasonic intensity, causing unsteady liquid surface resulting to a decreased sonochemical. However, a large gap between liquid height and ultrasonic irradiation distance can decrease the intensity of the propagated sound wave due to scattering caused by the large number of bubbles and attenuation. It can be understood more clearly by evaluating the relation below:

$$I = I_0 \exp(-2\alpha d) \quad (17)$$

where I is the ultrasonic intensity at some distance, d, from the source, I_0 is the ultrasonic intensity at source of the ultrasound, and α is the attenuation coefficient. Therefore, a sound wave with low ultrasonic intensity will be formed at higher liquid level. In addition, with increased height the hydrostatic pressure can act as a compressive pressure and suppress the groth of bubble. More about the optimum liquid height is explained by Kim et al. and the optimum value obtained in their research is shown in Fig. 5 [114].

So far, study on EC and US/EC oxidation of pollutants and its co-relation with liquid height have not been discussed. However, after seeing the above results on US and the relation of US with EC, an urgent need to explore this side of the study can be considered for an accurate design and development of the specific US/EC reactor.

8.5. Electrode material

Few important properties of electrode that should be covered are high stability, resistance to corrosion and passivating layer formation, high electrical conductivity, good catalytic activity and selectivity, low cost/life ratio etc. [115]. Electrode material determines the selectivity and the efficiency of a process. Moreover, greater the oxidation potential of an electrode material, the better is the degradation [116].

The anode material also influences the thermodynamic potential of $HO^{\cdot}$ formation, which is one of the reactive radicals responsible for pollutant oxidation. The thermodynamic standard potential for the free hydroxyl radical formation (Eq. (18)) can be calculated using the following Eq. (19):

$$HO^{\cdot}_{(aq)} + H^{+}_{(aq)} + e^{-} \leftrightarrow H_2O_{(l)} \quad (18)$$

$$E^{\circ} = -\frac{\Delta G^{\circ}_r}{zF} \quad (19)$$

where E° (V) is the standard thermodynamic potential of the reaction given, ΔG°_r (kJ mol^{-1}) is the standard Gibbs free energy of the

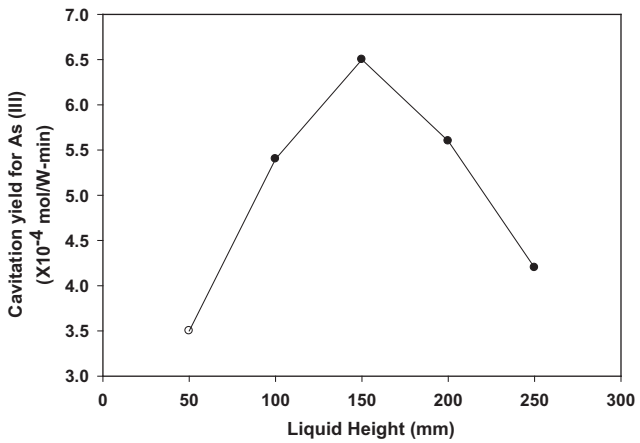

Fig. 5. Effect of the liquid height on cavitation yield for As (III) oxidation [114]. Experimental Condition: initial as (III) concentration: 1 mg/L, dimensions of the bottom plate of the sonoreactor: W 100 × L 226 mm^2, input power: 240 W, frequency: 334 kHz, reaction time 1 h.

reaction, z is the number of transferred electrons and F (C mol^{-1}) is the Faraday constant. The thermodynamic standard potential for OH$^{\cdot}$ is 2.38 V when the Gibbs energy of liquid water as −273.178 kJ mol^{-1} and that of hydroxyl radicals in the aqueous state as −7.74 k mol^{-1}, hence requiring higher anodic potentials for producing free hydroxyl radicals electrolytically.

According to the material and the interaction with reactive radicals, electrodes can be of two distinguished types. (a) Active electrocatalytic electrode signified by strong interaction between the electrode surface and hydroxyl radicals involves the partial (selective) oxidation of organics (eg. IrO_2). (b) Non-active, non-electrocatalytic electrode involves a weak interaction between the electrode surface and hydroxyl radicals. For non-active electrodes, the oxidation of organics occurs directly with hydroxyl radicals, resulting generally in a complete oxidation (eg. BDD). In addition, the EC activity (overpotential for oxygen evolution) and chemical reactivity (rate of organics oxidation) depends on the strength of electrode surface and hydroxyl radical interaction. If the interaction is weak the anode reactivity toward oxygen evolution is also weak and the anode reactivity for organic reaction (fast chemical reaction) is strong. Hence, in this context non active electrode like BDD is considered to be the best.

However, there are various other properties that also need to be considered. Besides, different materials hold different properties. For example, TiO_2 gives better mechanical stability, and when it is doped with other materials like RuO_2 and IrO_2, they have longer lifetime and higher electrochemical activity. Besides, it can be used as catalysts to explore the photo-mechanism involved in ultrasound and UV processes. Meanwhile, the incorporation of SnO_2 exhibits more stability and better resistance to corrosion. Iridium is also resistant to corrosion and is stable at high temperature. Its films are considered to have excellent electro-catalytic properties and good stability in strong acidic solution. Boron with its low charge carrier activation energy of only 0.37 eV makes BDD electrode a superconducting. If doped with a concentration between 500 and 1000 ppm, it is considered to give resistive power to corrosion [117].

The violent collapse of bubbles induced by the propagation of acoustic waves in a liquid medium at pressure may turn out to be a drawback for some US/EC degradation processes. The physical effects of these collapses, namely, high rates of micromixing, cleaning of electrodes' surfaces by dissolving or pitting the inhibiting layers; in the process of enhancing of the solid–liquid mass transfer between the electrodes and the solution may also lead to the erosion of fabricated electroactive layers reducing its efficient property.

Different electrode materials accompanied with their respective properties and pollutant degradation degrees are given in the Table 8, whereas Table 9 shows the efficiencies related to different electrodes.

8.6. Electrode size and electrode gap

The size and shape of the electrodes affect the surface area in contact. Larger surface areas provide more active EC oxidation sites [118]. The area of electrode is one of the important parameters determining the reactor performance through its quantitative relation of the space-time yield or weight of the product per unit time per unit volume of a reactor. It is determined along with other parameters, namely, current density and the current efficiency, which are again directly or indirectly related to and the area of electrode per unit volume of cell [119].

The space–time yield, Y_{ST} of a reactor is given in Eq. (20):

$$Y_{ST} = -\frac{iaM}{1000zF}CE \tag{20}$$

where i is current density, a is specific electrode area, z is charge number, F is Faraday constant and CE is current efficiency. The space–time yield gives an overall index of a reactor performance, especially the influence of the specific electrode area [24]. The availability of high area in three-dimensional electrode has been one good suggestion for an effective design of a compact reactor. However, such dimension does not allow an effective control on the reaction environment due to non-uniform fluid flow and change in the electrode potential. Hence, in many cases the use of porous and flow through electrodes has been recommended for better current efficiency [77].

In the case of small electrode, its smaller size decreases the signal-to-noise ratio and the small increment in the current of an electrode of smaller than 1 mm is due to greater waves affecting the turbulent movement [5]. Again, for ultramicrotrodes in the order of micrometers (between 0.8 and 50.0 μm), it has been claimed that, its dimensions are similar to those of the diffusion layer, resulting in a high-speed mass transport, due to the spherical

Table 8
Different modified electrodes with their respective oxidation potential and active component [118].

Active compound	Electrode	Oxidation potential (V)	Adsorption enthalpy of –OH	Oxidation power of anode
RuO_2	RuO_2-TiO_2 (DSA-Cl_2)	1.4–1.7	Chemisorption of OH radical	Low
IrO_2	IrO_2-Ta_2O_5 (DSA-O_2)	1.5–1.8		
Pt	Ti/Pt	1.7–1.9		
PbO_2	Ti/PbO_2	1.8–2.0		
SnO_2	Ti/SnO_2-Sb_2O_5	1.9–2.2		
BDD	p-Si/BDD	2.2–2.6	Physisorption of OH radical	High

Table 9
Details on direct anodic oxidation of organic compounds at different types of anode [77].

Anode	Pollutant	J, I or E (A/m^2)	Electrical efficiency (%)	Removal efficiency	Experiment condition
BDD	Phenol	100–300	100	5000–300 ppm	pH:7.0, electrolyte: 0.1 M Na_2CO_3
PbO_2	Glucose	100–900	30–60	100%	Electrolyte: H_2SO_2, T: 25–57 °C.
Pt	Ammonia	8.5	53	40%	pH: 8.2
Ti/BDD	Dyes	100	70–90	80–97%	pH: 4.7-6.7, T: 30 °C.
Ti/BDD, Ti/SnO_2-Sb_2O_3	Phenol	100	78.5	97% 64%	Electrolyte: Na_2SO_4 (2000 mg/L), T: 30 °C
Ti/IrO_2	Phenol	0.05	0.17	71%	pH > 9, T: 50
Ti/PbO_2	Landfill leachate	50–150	30	90%	pH: 8.3, conductivity: 12 mS/cm

Abbreviations: T: Temperature, J: Current Density, I = Current, E: Potential.

shape of the diffusion layer, which facilitates the conduction of EC reactions under steady state conditions achieved in a shorter time than with conventional electrodes [120].

On the other hand, a small interelectrode gap is recommended for low energy consumption. Greater the interelectrode distance, higher is the increase in ohmic potential drop; however, the distance must be maintained in such a way that there is no short circuit [121]. However, the electrodes are recommended to place in the region of acoustic streaming to enhance the mass transfer of electroactive compounds. Decreasing the electrode spacing decreases the internal resistance. In one case, an internal resistance was decreased 75% when the electrode spacing decreased from 3 to 1 cm, with values of 56 Ω (3-cm spacing), 34 Ω (2 cm), and 14 Ω (1 cm) [122]. In another study, the optimum distance between electrodes for sodium hypochlorite generation was 1 cm supporting the above explanation of the smaller electrode gap lower is the solution resistance between electrodes, increasing the production rate of O^{2-} or OH^- ions. Correspondingly, the rate of the reactions and the electric field intensity also become higher due to the smaller electrode gap. The Coulombic efficiency and energy recovery were also improved [123].

8.7. Applied voltage

The oxidation of water to produce reactive radicals occurs at approximately 1.2 V vs. NHE (normal hydrogen electrode). Therefore, a voltage higher than 1.2 V has to be applied for the EC oxidation of pollutants. Increasing the electric voltage also increases the electric current, thereby making it possible to degrade pollutants more. Besides, the thermodynamic equilibrium potential must be lower than the applied voltages due to polarization for the execution of an EC-oxidation system.

The distribution pattern of potential in the system can be known from Eq. (21) below:

$$V = \phi_{e,A} - \phi_{e,K} + |\Delta\phi_A| + |\Delta\phi_K| + \mathrm{IRL} + \mathrm{IRA} + \mathrm{IRK} \quad (21)$$

$\phi_{e,A}$ and $\phi_{e,K}$ are equilibrium potential of anode and cathode, respectively. $|\Delta\phi_A|$ and $|\Delta\phi_K|$ are the absolute value of anode overpotential and cathode overpotential, respectively. I is electric current. R_L is solution resistance. R_A and R_K are lead resistance to anode and to cathode, respectively.

Through the above equation, the application of electrolytic voltage can also be predicted. According to the work of Shen et al., the oxidation potential of graphite anode is 1.14 V versus *the Standard Hydrogen Electrode*. The current density of Acid Red B was calculated as 1.0 mA cm^{-2} on a graphite anode. Hence, logically 3 V, the sum potential of $\phi_{e,A}$ and $|\Delta\phi_A|$ should exceed 1.14 V. Therefore, the voltage should be 2–3 times higher in order to perform EC degradation. In the same study, 3.0 V was found to be optimum [124]. Xiong et al. also reported the existence of optimum voltage [125]. The existence of optimum applied voltage may be because initially, increased voltage favors the elimination of the passivized polymer film formed at the electrode surface thereby increasing the electrode active surface area. Consequently, mass transfer is increased and active desorption of the reaction products takes place increasing the kinetic rate constant. However, continuous increased in voltage increases the overpotential necessary for the production of oxidants and energy consumption becomes higher. Simultaneously, the service activity and lifetime of electrode is shortened [126].

On the contrary, Parsa et al. reported that after 120 min of EC-oxidation, the difference between the percent rate of COD removal for the applied voltage of 15 and 20 V was just 7%. However, in terms of energy consumption, a marked increase at 20 V was observed showing which cannot be regarded as advantageous to choose higher potential [127].

From the above cases, it can be recommended that choosing an efficient operating voltage from an economic point of view is also important. Besides, it is confirmed that the energy consumption increases with increased voltage which can be calculated from the relation the Eq. (22) given below:

$$W_{sp} = C_{sp} \times U\,(\mathrm{kWh\ dm^{-3}}) \quad (22)$$

where W_{sp} is specific energy consumption and C_{sp} represents the specific charge consumption of C corresponding to 1 dm^3 and U is the cell voltage (V) [128]. However, the consumption of energy by using high voltage can be reduced by incorporating electrolytes. Adding electrolyte like NaCl increases the conductivity and decreases the ohmic resistance of wastewater, thereby reducing the cell voltage V at a constant current density [129,130,131].

8.8. Current density distribution

Current density is also among the indisputable parameters controlling the reaction rate. Depending on the applied current density (i_{appl}) and limited current density (i_{lim}), two different operating regimes can be identified i.e., $i_{appl} < i_{lim}$ where the electrolysis is under current control with the current efficiency of 100% and when $i_{appl} > i_{lim}$ the electrolysis is under mass-transport control and the secondary reactions of oxygen evolution are involved with a decreasing of current efficiency. However, the application of right i_{appl} lies on the electrochemical efficiency contemplating both the limitations of electrode fouling and electrical charge consumption [68,132]. Practically, higher current density results in an intensification of the temperature of the reaction solution directing to a proportional increase of the applied potential and then high consumption of power [133]. However, when similar method like US is combined, the current efficiency has been found to be advantageous.

In a work done by Wu et al. using 100 mg/L CI Reactive Black 8, initial pH 5.4, 0.1 mol/L Na_2SO_4 and 100 W/L acoustic power, the decolorization of CI Reactive Black 8 was found to enhance by the EC with US process. The decolorization rate constants for 15.9, 31.7–47.6 mA cm^{-2} for the EC process were 0.0056, 0.0085 and 0.0123 min^{-1} respectively. However for the combined US/EC process, the rates were 0.0072, 0.0103, and 0.0133 min^{-1}, respectively. The enhancement factor, f shown by the equation, $f = \frac{k_{US/EC}}{k_{EC}}$, were 1.28, 1.21 and 1.08 for 15.9, 31.7 and 47.6 m cm^{-2} of current density, respectively. When anodic oxidation alone was accounted, CI Reactive Black 8 was destroyed by the hydroxyl radical electrogenerated at the surface of high oxygen overvoltage anode through the following water dissociation as in Eq. (23):

$$H_2O \rightarrow H^+ + {}^{\cdot}OH + e^- \quad (23)$$

With the increase in current density, the production of hydroxyl radicals from water oxidation is also expected to increase, which again is enhanced by its combination with US. However, it has to be taken into consideration that for higher current density higher specific electrical charge passed is the EC oxidation, the aspect that limited its application from the economic consideration [134]. Hence, considering the energy consumption, Jiade et al., concluded 15 mA/cm^2 as optimum among the 5, 10, 15 and 20 mA/cm^2 studied for the electrochemical degradation of chlorobenzene [135]. Nevertheless, it can again be reduced by employing a catalyst [136].

Leite et al. investigated the US/EC-degradation of 300 mg/L 2,4-dihydroxybenzoic acid (2,4-DHBA) by potentiostatic and galvanostatic electrolyses on platinum electrode. When 300 Am^{-2} current density was applied, at 20 kHz, the TOC removal was 47% after passing an electricity amount of 1.5 Ah and at 500 kHz, 32% after passing 3.5 Ah. The electrochemical energy efficiency at low

frequency was greater than at high frequency but in both cases, the overall energy consumption is reported to be high which is greater than 200 Wh kg^{-1} [21]. Hence, in the case of current density, a compromise between maximum oxidation rate and minimum energy consumption is necessary. With limited research available as of now on this particular topic, alternatives recommended till now are either carrying multiple step EC-oxidations or incorporating a catalyst in the electric field [137,138].

8.9. Conclusion and future perspectives

Although this field has received much attention over the past decade, there is no large scale standardized arrangement, except for few generic experimental arrangements at smaller scale or laboratory scale. The traditional arrangement of the ultrasonic probe placing above an electrode is still widely used, indicating a sluggish development and slow evolution in reactor configuration studies. More scientific studies based on the refinements to the operation and geometries; with deeper emphasis on cost analysis is a must. The studies should be accompanied by proper evaluation of its effectiveness and possible side effects need to be performed in order to make it acceptable to the mass. Besides, rigorous research and development to provide better understanding of the mechanisms; measurements of the efficiency of the candidate processes under controlled experimental conditions; realistic evaluations of the relative costs of candidate processes for selected treatment objectives versus other treatment processes; evaluation of by-products and their toxicity; reliability factors for candidate processes etc. need to be conducted.

Further, in depth optimization based on reactor configuration for the enhancement of system is recommended. Among the design, the extent of cavitation, either stable or transient, and the maximum contact between the pollutant and reactive radical should be prioritized. Equal importance should be given on the electrode parameters to increase both direct and indirect mechanisms. It can further extend to kinetic rate modeling under the influence of critical parameters like concentration, temperature, etc. Other researchers have also suggested a need for an optimum ratio of electrode area to reaction volume in an experimental gap reactor. This will enable a preparative scale US/EC and provide further information on suitable reactor design, operation parameters and yield depending on US settings and current density. Besides, by optimizing such configurations, the intensity of cavitation formation as well as its impact on the electrode and production of reactive radicals will be higher. On the other hand, effective optimization of the distance between the ultrasonic horn and the working electrode on the current density should be evaluated and compared with the results of a basic modeling of the sound field. The distance between these two parameters will be a crucial aspect in the expected synergism and hence it is recommended to establish keeping in mind both the theoretical simulations and experimental analysis.

Designing of process intensifying parameters like catalyst and synthesis of stable catalytic electrodes are among the challenges that can be taken up. Here the influence of ultrasonic mechanical phenomena such as acoustic streaming, turbulence, etc. is needed to be cautious to maintain the durability of the synthesized material throughout the process operation. However, use of non-active, highly conductive materials such as BDD electrodes is also considered to be the most economical technique for increasing the impact of reactive radical production.

Quantification of bubble formation and its relation to electrolytic reaction enhancement, taking note of the influencing parameters like power dissipation and frequency of irradiation for the production of more reactive radicals should be taken up through both theoretical and practical approaches. Adoption of radical measurement methods like Potassium Iodide Dosimetry or development of new engineering equations, etc. can be among alternative suggestion.

Besides, the main limitation is its energetic cost. Hence different strategies should be built like lowering the ultrasonic intensity or using pulsed mode. Proper electrode material should also be selected for optimization of acoustic field from US/EC point of view. From a bigger approach, coupling with other advance oxidation processes may give rise to a more efficient decontamination such as in electro-oxidation with sonophotocatalysis or combining with ozonation which few have recently proposed. Moreover, the combination with bulk oxidation processes such as Fenton reagent is also highly effective considering the mechanisms that can be activated in the presence of ultrasound, therefore eliminating the drawbacks of the individual techniques by the characteristics of other technique.

The effects of US on an EC process remain a largely unexplored area, though many researchers suggested its significant benefits. New tools are needed to develop for segregation of its chemical effects from real physical form of mass transport, thermal effects, etc. Thermodynamics equations can be explored in such studies. Through it, predictions of electrolytic parameters like voltage, current intensity, etc. can also be made. Overall, a true optimization of such combined oxidation system requires contributions from many disciplines including physics, fundamental and applied EC, chemical engineering etc.

Acknowledgements

This work was supported by the Basic Science Research Program through a National Research Foundation of Korea (NRF) grant funded by the Ministry of Education, Science and Technology (KRF-2009-0092799) and research scholarship provided by National Institute for International Education (NIIED), Ministry of Education, South Korea.

References

[1] A. Yaqub, H. Ajab, Applications of sonoelectrochemistry in wastewater treatment system, Rev. Chem. Eng. 29 (2013) 123–130.
[2] S.K. Sharma, R. Sanghi, Advances in water treatment and pollution prevention, Springer Sci. C Bus. Media, Dordrecht, 2012.
[3] A.A. Zorpas, I. Voukalli, P. Loizia, Chemical treatment of polluted waste using different coagulants, Desalin. Water Treat. 45 (2012) 291–296.
[4] F. Trabelsi, H.A. Lyazidi, B. Atsimba, A.M. Wilhelm, H. Delmas, P.L. Fabre, J. Berlan, Oxidation of phenol in wastewater by sonoelectrochermistry, Chem. Eng. Sci. 51 (1996) 1857–1865.
[5] J. Klima, Application of ultrasound in electrochemistry. An overview of mechanisms and design of experimental arrangement, Ultrasonics 51 (2011) 202–209.
[6] J.G. Garcia, M.D. Esclapez, P. Bonete, Y.V. Hernandez, L.G. Garreton, V. Saez, Current topics on Sonoelectrochemistry, Ultrasonics 50 (2010) 318–322.
[7] N. Morigushi, The effect of supersonic waves on chemical phenomena, (III). The effect on the concentration polarization, J. Chem. Soc. Jpn 55 (1934) 749–750.
[8] E. Yeager, F. Kovorka, J. Dereska, Effects of acoustical waves on the electrodeposition of chromium, J. Acoust. Soc. Am. 29 (1957) 769.
[9] A.J. Bard, High speed controlled potential coulometry, Anal. Chem. 35 (1963) 1125–1128.
[10] S. Eren, L. Toppare, U. Akbulut, Electro initiated cationic copolymerization of 4-bromostyrene and α-methylstyrene in the presence of ultrasonic vibration, Polym. Commun. 28 (1987) 36–38.
[11] S. Osawa, M. Ito, K. Tanaka, J. Kuwano, Electrochemical polymerization of thiophene under ultrasonic field, Synth. Met. 18 (1987) 145–150.
[12] D.J. Walton, J. Iniesta, M. Plattes, T.J. Mason, J.P. Lorimer, S. Ryley, A. Chyla, J. Heptinstall, T. Thiemann, H. Fuji, S. Mataka, Y. Tanaka, Sonoelectrochemical effects in electro-organic systems, Ultrason. Sonochem. 10 (2003) 209–216.
[13] A. Chyla, J.P. Lorimer, T.J. Mason, G. Smith, D.J. Walton, Modifying effect of ultrasound upon the electrochemical oxidation of cyclohexanecarboxylate, J. Chem. Soc., Chem. Commun. (1989) 603–604.
[14] Y. Ono, Y. Nishiki, T. Nonaka, Electrolysis using composite plated electrodes. Preparation of a binary type composite plated nickle electrode with poly(tetrafluoroethylene) and sili gel and its application in electroreduction of aldehydes, Chem. Lett. (1994) 1623.

[15] R.G. Compton, J.C. Eklund, F. Marken, Sonoelectrochemical process: a review, Electroanalysis 9 (1997) 509.
[16] T.J. Mason, J.P. Lorimer, D.J. Walton, Sonoelectrochemistry, Ultrasonics 28 (1990) 333–337.
[17] V. Yegnaraman, S. Bharathi, Sonoelectrochemistry-an emerging area, Bull. Electrochem. 8 (1992) 84–85.
[18] J.P. Lorimer, T.J. Mason, M. Plattes, S.S. Phull, Dye effluent decolourisation using ultrasonically assisted electro-oxidation, Ultrason. Sonochem. 7 (2000) 237–242.
[19] J.S. Foord, K.B. Holt, R.G. Compton, F. Marken, D.H. Kim, Mechanistic aspects of the sonoelectrochemical degradation of the reactive dye Procion Blue at boron-doped diamond electrodes, Diamond Relat. Mater. 10 (2001) 662–666.
[20] M.E. Abdelsalam, P.R. Birkin, A study investigating the sonoelectrochemical degradation of an organic compound employing Fenton's reagent, Phys. Chem. 4 (2002) 5340–5345.
[21] R.H.L. Leite, P. Cognet, A.M. Wilhelm, H. Delmas, Anodic oxidation of 2,4-dihydroxybenzoic acid for wastewater treatment: study of ultrasound activation, Chem. Eng. Sci. 57 (2002) 767–778.
[22] Y. Yasman, V. Bulatov, V.V. Gridin, S. Agur, N. Galil, R. Armon, I. Schechter, A new sono-electrochemical method for enhanced detoxification of hydrophilic chloroorganic pollutants in water, Ultrason. Sonochem. 11 (2004) 365–372.
[23] R.C. Alkire, S. Perusich, The effect of focused ultrasound on the electrochemical passivity of iron in sulfuric-acid, Corros. Sci. 23 (1983) 1121–1132.
[24] J. González-Garcíaa, V. Sáeza, M.D. Esclapeza, P. Bonetea, Y. Vargasb, L. Gaeteb, Relevant developments and new insights on Sonoelectrochemistry, Phys. Proc. 3 (2010) 117–124.
[25] H. Zhang, L.A. Coury Jr, Effects of high-intensity ultrasound on glassy-carbon electrodes, Anal. Chem. 65 (1993) 1552–1558.
[26] R.G. Compton, J.C. Eklund, S.D. Page, G.H.M. Sanders, J. Booth, Voltammetry in the presence of ultrasound - sonovoltammetry and surface effects, J. Phys. Chem. 98 (1994) 12410–12414.
[27] D.J. Walton, S.S. Phull, A. Chyla, J.P. Lorimer, L.D. Burke, M. Murphy, R.G. Compton, J.C. Eklund, S.D. Page, Sonovoltammetry at platinum electrodes: surface phenomena and mass transport processes, J. Appl. Electrochem. 25 (1995) 1083–1090.
[28] F. Marken, R.G. Compton, Electrochemistry in the presence of ultrasound: the need for bipotentiostatic control in sonovoltammetric experiments, Ultrason. Sonochem. (1996) S131–S134.
[29] R.G. Compton, J.C. Eklund, F. Marken, D.N. Waller, Electrode processes at the surfaces of sonotrodes, Electrochim. Acta 41 (1996) 315–320.
[30] E.L. Cooper, L.A. Coury Jr, Mass transport in sonovoltammetry with evidence of hydrodynamic modulation from ultrasound, J. Electrochem. Soc. 145 (1998) 1994–1999.
[31] K. Macounova, J. Klima, C. Bernard, C. Degrand, Ultrasound-assisted anodic oxidation of diuron, J. Electroanal. Chem. 457 (1998) 141–147.
[32] C.H. Goeting, J.S. Foord, F. Marken, R.G. Compton, Sonoelectrochemistry at tungsten-supported boron-doped CVD diamond electrodes, Diamond Relat. Mater. 8 (1999) 824–829.
[33] A.J. Saterlay, C. Agra-Gutierrez, M.P. Taylor, F. Marken, R.G. Compton, Sono-cathodic stripping voltammetry of lead at a polished boron-doped diamond electrode: application to the determination of lead in river sediment, Electroanal. 11 (1999) 1083–1088.
[34] J.L. Hardcastle, R.G. Compton, Sonoelectroanalytical determination of heavy metals in fish gill mucous, Electroanalysis 13 (2001) 89–93.
[35] J.S. Foord, K.B. Holt, R.G. Compton, F. Marken, D.H. Kim, Mechanistic aspects of the sonoelectrochemical degradation of the reactive dye procion blue at boron-doped diamond electrodes, Diam. and Relat. Mater. 10 (2001) 662–666.
[36] K.B. Holt, C. Forryan, R.G. Compton, J.S. Foord, F. Marken, Anodic activity of boron-doped diamond electrodes in bleaching processes: effects of ultrasound and surface states, New J. Chem. 27 (2003) 698–703.
[37] G.S. Garbellini, G.R. Salazar-Banda, L.A. Avaca, Sonovoltammetric determination of 4-nitrophenol on diamond electrodes, J. Braz. Chem. Soc. 18 (2007) 1095–1099.
[38] G.H. Zhao, S.H. Shen, M.F. Li, M.F. Wu, T.C. Cao, D.M. Li, The mechanism and kinetics of ultrasound-enhanced electrochemical oxidation of phenol on boron-doped diamond and Pt electrodes, Chemosphere 73 (2008) 1407–1413.
[39] G.S. Garbellini, G.R. Salazar-Banda, L.A. Avaca, Sonovoltammetric determination of toxic compounds in vegetables and fruits using diamond electrodes, Food Chem. 116 (2009) 1029–1035.
[40] M.D. Esclapez, V. Saez, D. Milán-Yáñez, I. Tudela, O. Louisnard, J. González-García, Sonoelectrochemical treatment of water polluted with trichloroacetic acid: from sonovoltammetry to pre-pilot plant scale, Ultrason. Sonochem. 17 (2010) 1010–1020.
[41] X. Zhu, J. Ni, H. Li, Y. Jiang, X. Xing, A.G.L. Borthwick, Effects of ultrasound on electrochemical oxidation mechanisms of p-substituted phenols at BDD and PbO_2 anodes, Electrochim. Acta 55 (2010) 5569–5575.
[42] M. Siddique, R. Farooq, Z.M. Khan, Z. Khan, S.F. Shaukat, Enhanced decomposition of reactive blue 19 dye in ultrasound assisted electrochemical reactor, Ultrason. Sonochem. 18 (2011) 190–196.
[43] E. Neyens, J. Baeyens, A review of classic Fenton's peroxidation as an advanced oxidation technique, J. Hazard. Mater. 98 (2003) 33–50.
[44] B. Brown, J.E. Goodman, High intensity ultrasonics, Iliffe Books, 1956.
[45] H.M. Han, G.J. Phillips, S.V. Mikhalovsky, S. FitzGerald, A.W. Lloyd, Sonoelectrochemical deposition of calcium phosphates on carbon materials: effect of current density, J. Mater. Sci. - Mater. Med. 19 (2008) 1787–1791.
[46] K.R. Murali, P. Sasindran, Structural and optical properties of sonoelectrochemically deposited CdSe films, J. Mater. Sci. 39 (2004) 6347–6348.
[47] A.J. Saterlay, S.J. Wilkins, Ch.H. Goeting, J.S. Foord, R.G. Compton, F. Marken, Sonoelectrochemistry at highly boron-doped diamond electrodes: silver oxide deposition and electrocatalysis in the presence of ultrasound, J. Solid State Electrochem. 4 (2000) 383–389.
[48] B. Pollet, J.P. Lorimer, S.S. Phull, J.Y. Hihn, Sonoelectrochemical recovery of silver from photographic processing solutions, Ultrason. Sonochem. 7 (2000) 69–76.
[49] S.K. Mohapatra, K.S. Raja, M. Misra, V.K. Mahajan, M. Ahmadian, Synthesis of self-organized mixed oxide nanotubes by sonoelectrochemical anodization of Ti–Mn alloy, Electrochim. Acta 53 (2007) 590–597.
[50] J. Kang, Y. Shin, Y. Tak, Growth of etch pits formed during sonoelectrochemical etching of aluminium, Electrochim. Acta 51 (2005) 1012–1016.
[51] D. Reyman, E. Guereca, P. Herasti, Elecrodeposition of polythiophene assisted by sonochemistry and incorporation of fluorophores in the polymetric matrix, Ultrason. Sonochem. 14 (2007) 653–660.
[52] C.W. Lee, R.G. Compton, J.C. Eklund, D.N. Waller, Mercury-electroplated platinum electrodes and microelectrodes for sonoelectrochemistry, Ultrason. Sonochem. 2 (1995) S59–S62.
[53] M.A. Murphy, F. Marken, J. Mocak, Sonoelectrochemistry of molecular and colloidal redox systems at carbon nanofiber–ceramic composite electrodes, Electrochim. Acta 48 (2003) 3411–3417.
[54] J. Kolb, W. Nyborg, Small-scale acoustic streaming in liquids, J. Acoust. Soc. Am. 28 (1956) 1237–1242.
[55] R.G. Compton, J.L. Hardcastle, J. del Campo, Sonoelectroanalysis: applications, in: Bard-Stratmann (Ed.), Encyclopedia of Electrochemistry, in: Pat Unwin (Ed.), Instrum. Electrochem. Chem. 3 (2003) 312–327.
[56] J.C. Ball, R.G. Compton, Application of ultrasound to electrochemical measurements and analyses, Electrochemistry (Tokyo) 67 (1999) 912–919.
[57] J.D. Wadhawan, F. Marken, R.G. Compton, Biphasic sonoelectrosynthesis. A review, Pure Appl. Chem. 73 (2001) 1947–1955.
[58] H.S. Fogler, Ultrasonic gas absorption and acoustic streaming observations, Chem. Eng. Prog. Symp. 67 (109) (1971) 1.
[59] I. Haas, S. Shanmugam, A. Gedanken, Pulsed sonoelectrochemical synthesis of size-controlled copper nanoparticles stabilized by poly(N-vinylpyrrolidone), J. Phys. Chem. B 110 (2006) 16947–16952.
[60] I. Haas, A. Gedanken, Synthesis of metallic magnesium nanoparticles by b sonoelectrochemistry, Chem. Commun. 15 (2008) 1795–1797.
[61] H. Lei, Y.J. Tang, J.J. Wei, J. Li, X.B. Li, H.L. Shi, Synthesis of tungsten nanoparticles by sonoelectrochemistry, Ultrason. Sonochem. 14 (2007) 81–83.
[62] Y.Ch. Liu, L.H. Lin, W.H. Chiu, Size-controlled synthesis of gold nanoparticles from bulk gold substrates by sonoelectrochemical methods, J. Phys. Chem. B. 108 (2004) 19237–19240.
[63] Y.Ch. Liu, L.H. Lin, New pathway for the synthesis of ultrafine silver nanoparticles form bulk silver substrates in aqueous solutions by sonoelectrochemical methods, Electrochem. Commun. 6 (2004) 1163–1168.
[64] M. Luan, G. Jing, Y. Piao, D. Liu, L. Jin, Treatment of refractory organic pollutants in industrial wastewater by wet air oxidation, Arabian J. Chem. (2012) 1878–5352.
[65] B. Thokchom, K. Kim, J. Park, J. Khim, Ultrasonically enhanced electrochemical oxidation of ibuprofen, Ultrason. Sonochem. 22 (2015) 429–436.
[66] H.S. Awad, N.A. Galwa, Electrochemical degradation of acid blue and basic brown dyes on Pb/PbO_2 electrode in the presence of different conductive electrolyte and effect of various operating factors, Chemosphere 9 (2005) 1327–1335.
[67] J.L. Hardcastle, J.C. Ball, Q. Hong, F. Marken, R.G. Compton, S.D. Bull, S.G. Davies, Sonoelectrochemical and sonochemical effects of cavtation: correlation with interfacial cavitation induced by 20 kHz ultrasound, Ultrason. Sonochem. 7 (2000) 7–14.
[68] M.A. Rodrigo, P.A. Michaud, I. Duo, M. Panizza, G. Cerisola, Comninellis, oxidation of 4-chlorophenol at boron-doped diamond electrode for wastewater treatment, J. Electrochem. Soc. 148 (2001) 60–64.
[69] G.S. Garbellini, G.R. Salazar-Banda, L.A. Avaca, Effects of ultrasound on the degradation of pentachlorophenol by boron-doped diamond electrodes, Portugaliae Electrochim. Acta 28 (2010) 405–415.
[70] Waste treatment by sonochemical, electrochemical and sonoelectrochemical technology. SGITT-OTRI (University of Alicante), <http://sgitt-otri.ua.es/es/empresa/ofertas-tecnologicas.html>.
[71] T. Abid, S.N. Khan, N. Hussain, M. Siddique, Q. Mahmood, I. Hussain, F. Mateen, Z. Ahmad, S.F. Shaukat, R. Farooq, Electrolyte assisted sono-electrochemical decomposition of reactive red 195, J. Chem. Soc. Pak. (2013) 377–384.
[72] Y.Z. Ren, Z.L. Wu, M. Franke, P. Braeutigam, B. Ondruschka, D.J. Comeskey, P.M. King, Sonoelectrochemical degradation of phenol in aqueous solutions, Ultrason. Sonochem. 20 (2013) 715–721.
[73] Y.G. Adewuyi, Sonochemistry in Environmental Remediation. 1. Combinative and hybrid sonophotochemical oxidation processes for the treatment of pollutants in water, Environ. Sci. Technol. 39 (2005) 3409–3420.
[74] K.S. Suslick, Sonochemistry, Sci. 247 (1990) 1439.

[75] D.J. Walton, Sonoelectrochemistry – the application of ultrasound to electrochemical systems, Arkivoc 3 (2002) 198.
[76] K.B. Holt, J.D. Campo, J.S. Foord, R.G. Compton, F. Marken, Sonoelectrochemistry at platinum and boron-doped diamond electrodes: achieving 'fast mass transport' for 'slow diffusers', J. Electroanal. Chem. 513 (2001) 94–99.
[77] A.M.H. Carlos, S. Ferro, Electrochemical oxidation of organic pollutants for the wastewater treatment: direct and indirect processes, Chem. Soc. Rev. 35 (2006) 1324–1340.
[78] I.C. Eloy, R. Catalina, A.M.H. Carlos, M.P.H. Juan, On-site hydrogen peroxide production at pilot flow plant: application to electro-fenton process, Int. J. Electrochem. Sci. 8 (2013) 3084–3094.
[79] M.E. Abdelsalam, P.R. Birkin, A study investigating the sonoelectrochemical degradation of an organic compound employing Fenton's reagent, Phys. Chem. Chem. Phys. 4 (2002) 5340–5345.
[80] M.A. Oturan, I. Sirés, N. Oturan, S. Pérocheau, J.L. Laborde, S. Trévin, Sonoelectro-Fenton process: a novel hybrid technique for the destruction of organic pollutants in water, J. Electroanal. Chem. 624 (2008) 329–332.
[81] A. Babuponnusamia, K. Muthukumarb, Advanced oxidation of phenol: a comparison between Fenton, electro-Fenton, sono-electro-Fenton and photo-electro-Fenton processes, Chem. Eng. J. 183 (2012) 1–9.
[82] H. Li, H. Lei, Q. Yua, Z. Li, X. Fenga, B. Yanga, Effect of low frequency ultrasonic irradiation on the sonoelectro-Fenton degradation of cationic red X-GRL, Chem. Eng. J. 160 (2010) 417–422.
[83] S.S. Martinez, E.V. Uribe, Enhanced sonochemical degradation of azure B dye by the electro Fenton process, Ultrason. Sonochem. 19 (2012) 174–178.
[84] S. Sahinkaya, COD and color removal from synthetic textile wastewater by ultrasound assisted electro-Fenton oxidation process, J. Ind. Eng. Chem. 19 (602) (2013) 601–605.
[85] Z. Zhang, Y. Yuan, L. Liang, Y. Fang, Y. Cheng, H. Ding, G. Shi, L. Jin, Sonophotoelectrocatalytic degradation of azo dye on TiO2 nanotube electrode, Ultrason. Sonochem. 15 (2008) 370–375.
[86] V.O. Abramov, A.E. Gekhman, V.M. Kuznetsov, G.J. Price, Ultrasonic intensification of ozone and electrochemical destruction of 1,3-dinitrobenzene and 2,4-dinitrotoluene, Ultrason. Sonochem. 13 (2006) 303–307.
[87] M. Rivera, M. Pazos, M.A. Sanroman, Improvement of dye electrochemical treatment by combination with ultrasound technique, J. Chem. Technol. Biotechnol. 84 (2009) 1118–1124.
[88] Z. Ai, J. Li, L. Zhang, S. Lee, Rapid decolorization of azo dyes in aqueous solution by an ultrasound-assisted electrocatalytic oxidation process, Ultrason. Sonochem. 17 (2010) 370–375.
[89] S.N. Giray, D. Aktas, M. Dolaz, Y. Uysal, Removal of dye from real textile wastewater by sono-electro-Fenton oxidation process, J. Selcuk University Nat Appl. Sci. (2014). Online ISSN: 2147–3781 (Digital Proceeding of the ICOEST).
[90] E. Bringas, J. Saiz, I. Ortiz, Kinetics of ultrasound-enhanced electrochemical oxidation of diuron on boron-doped diamond electrodes, Chem. Eng. J. 172 (2011) 1016–1022.
[91] M.P. Titus, V.G. Molina, M.A. Baños, J. Giménez, S. Esplugas, Degradation of chlorophenols by means of advanced oxidation processes: a general review, Appl. Cat. B: Environ. 47 (2004) 219–256.
[92] A. Durant, H. Francois, J. Reisse, A.K. Demesmaeker, Sonoelectrochemistry: the effects of ultrasound on organic electrochemical reduction, Electrochim. Acta 41 (1996) 277–284.
[93] A. Lindermeir, C. Horst, U. Hoffmann, Ultrasound assisted electrochemical oxidation of substituted toluenes, Ultrason. Sonochem. 10 (2003) 223–229.
[94] G. Zhao, J. Gao, S. Shen, M. Liu, D. Li, M. Wu, Y. Lei, Ultrasound enhanced electrochemical oxidation of phenol and phthalic acid on boron-doped diamond electrode, J. Hazard. Mater. 172 (2009) 1076–1081.
[95] V. Sáez, M.D. Esclapez, I. Tudela, P. Bonete, O. Louisnard, J.G. García, 20 kHz sonoelectrochemical degradation of perchloroethylene in sodium sulfate aqueous media: influence of the operational variables in batch mode, J. Hazard. Mat. 183 (2010) 648–654.
[96] V. Sáez, I. Tudela, M.D. Esclapez, P. Bonete, O. Louisnard, J.G. García, Sonoelectrochemical degradation of perchloroethylene in water: enhancement of the process by the absence of background electrolyte, Chem. Eng. J. 168 (2011) 649–655.
[97] G. Yildiz, H.C. Giz, A. Giz, Effect of ultrasound on electrochemically initiated acrylamide polymerization, J. Appl. Polym. Sci. 84 (2002) 83–89.
[98] T. J. Mason, J. P. Lorimer, Applied Sonochemistry: The Uses of Power Ultrasound in Chemistry and Processing, Weinheim, Germany, 2002.
[99] F.P. Capote, M.D. Luque de Castro, Analytical uses of ultrasound I. Sample preparation, Trends Anal. Chem. 23 (2004).
[100] B. Yang, J. Zuo, X. Tang, F. Liu, X. Yu, X. Tang, H. Jiang, L. Gan, Effective ultrasound electrochemical degradation of methylene blue wastewater using a nanocoated electrode, Ultrason. Sonochem. 21 (2014) 1310–1317.
[101] M. Sivakumar, A.B. Pandit, Ultrasound enhanced degradation of Rhodamine B: optimization with power density, Ultrason. Sonochem. 8 (2001) 233–240.
[102] B.G. Pollet, J.P. Lorimer, J.Y. Hihn, S.S. Phull, T.J. Mason, D.J. Walton, The effect of ultrasound upon the oxidation of thiosulphate on stainless steel and platinum electrodes, Ultrason. Sonochem. 9 (2002) 267–274.
[103] R. Molinari, F. Pirillo, V. Loddo, L. Palmisano, Heterogeneous photocatalytic degradation of pharmaceuticals in water by using polycrystalline TiO_2 and a nanofiltration membrane reactor, Catal. Today 118 (2006) 205–213.
[104] N. Golash, P.R. Gogate, Degradation of dichlorvos containing wastewaters using sonochemical reactors, Ultrason. Sonochem. 19 (2012) 1051–1060.
[105] P.R. Gogate, V.S. Sutkar, A.B. Pandit, Sonochemical reactors: important design and scale up considerations with a special emphasis on heterogeneous systems, Chem. Eng. J. 166 (2011) 1066–1082.
[106] F. R. Young, Cavitation McGraw-Hill Book Company, Maidenhead, UK, 1989, 40–76.
[107] A. Tiehm, K. Nickel, M. Zellhorn, U. Neis, Ultrasonic waste activated sludge disintegration for improving anaerobic stabilization, Water Res. 35 (2001) 2003–2009.
[108] P.A. Tatake, A.B. Pandit, Modelling and experimental investigation into cavity dynamics and cavitational yield: influence of dual frequency ultrasound sources, Chem. Eng. Sci. 57 (2002) 4987–4995.
[109] Y. Son, M. Lim, M. Ashokkumar, J. Khim, Geometric optimization of sonoreactors for the enhancement of sonochemical activity, J. Phys. Chem. C 115 (2011) 4096–4103.
[110] V. Renaudin, N. Gondrexon, P. Boldo, C. Petrie, A. Bernis, Y. Gonthier, Method for determining the chemically active zones in a high-frequency ultrasonic reactor, Ultrason. Sonochem. 1 (1994) S81–S85.
[111] Y. Kojima, S. Koda, H. Nomura, Effects of sample volume and frequency on ultrasonic power in solutions on sonication, Jpn. J. Appl. Phys. 37 (1998) 2992–2995.
[112] Y. Asakura, T. Nishida, T. Matsuoka, S. Koda, Effects of ultrasonic frequency and liquid height on sonochemical efficiency of large-scale sonochemical reactors, Ultrason. Sonochem. 15 (2008) 244–250.
[113] Y. Asakura, M. Maebayashi, T. Matsuoka, S. Koda, Characterization of sonochemical reactors by chemical dosimetry, Electron. Commun. Jpn. (Part III: Fundam. Electron. Sci.) 90 (2007) 1–8.
[114] E. Kim, M. Cui, M. Jang, B. Park, Y. Son, J. Khim, Investigation of sonochemical activities at a frequency of 334 kHz: the effect of geometric parameters of sonoreactor, Ultrason. Sonochem. 21 (2014) 1504–1511.
[115] A. Anglada, A. Urtiaga, I. Ortiz, Contributions of electrochemical oxidation to waste-water treatment: fundamentals and review of applications, J. Chem. Technol. Biotechnol. 84 (2009) 1747–1755.
[116] R. Parsons, Standard potentials in aqueous solution, Marcel Dekker, INC., 1985.
[117] J. Haore, Standard potentials in aqueous solution, Marcel Dekker, INC., 1985.
[118] P.S. Patela, N. Bandrea, A. Sarafa, J.P. Ruparelia, Electro-catalytic materials (electrode materials) in electrochemical wastewater treatment, Proc. Eng. 51 (2013) 430–435.
[119] A. Carlos, M. Huitle, S. Ferro, Electrochemical oxidation of organic pollutants for the wastewater treatment: direct and indirect processes, Chem. Soc. Rev. 35 (2006) 1324–1340.
[120] H. Xu, A. Li, X. Cheng, Electrochemical performance of doped SnO_2 coating on Ti base as electrooxidation anode, Int. J. Electrochem. Sci. 6 (2011) 5114–5124.
[121] S. Klamklang, H. Vergnes, K. Pruksathorn, S. Damronglerd, Electrochemical incineration of organic pollutants for wastewater treatment: past, present and prospect, Organic Pollutants Ten Years After the Stockholm Convention – Environmental and Analytical Update.
[122] G. Chen, Electrochemical technologies in wastewater treatment, Sep. Purif. Technol. 38 (2004) 11–41.
[123] A.N. Correia, L.H. Mascaro, S.A.S. Machado, L.H. Mazo, L.A. Avaca, Ultramicroeletrodos. Part 1: Revisão Teórica e Perspectivas, Quim. Nova 18 (1995) 475–480.
[124] L.K. Wang, Y.T. Hung, N.K. Shammas, Advanced physicochemical treatment technologies, Handb. Environ. Eng. 5 (2007) 710.
[125] Shoancheng, Hongliu, B. Logan, Increased power generation in a continuous flow MFC with advective flow through the porous anode and reduced electrode spacing, Environ. Sci. Technol. 40 (2006) 2426–2432.
[126] S.K. Sharma, Green Chemistry for Dyes Removal from Waste Water: Research Trends and Applications, Willey Publication 1 (2015) 496.
[127] M. Wang, L. Jia, S. Deng, Influence of anode area and electrode gap on the morphology of nanotubes arrays, J. Nanomat. (2013) 7.
[128] Z.M. Shen, D. Wu, J. Yang, T. Yuan, W.H. Wang, J.P. Jia, Methods to improve the electrochemical treatment effect of dye wastewater, J. Hazard. Mat. B131 (2006) 90–97.
[129] Y. Xiong, P.J. Strunk, H. Xia, X. Zhu, H.T. Karlsson, Treatment of dye wastewater containing acid orange II using a cell with three-phase three-dimensional electrode, Wat. Res. 35 (2001) 4226–4230.
[130] J.B. Parsa, M. Rezaei, A.R. Soleymani, Electrochemical oxidation of an azo dye in aqueous media investigation of operational parameters and kinetics, J. Hazard. Mat. 168 (2009) 997–1003.
[131] N. Daneshvar, A. Oladegaragoze, N. Djafarzadeh, Decolorization of basic dye solutions by electrocoagulation: an investigation of the effect of operational parameters, J. Hazard. Mat. 129 (2006). 116–112.
[132] X.M. Chen, G. Chen, P.L. Yue, Investigation on the electrolysis voltage of electrocoagulation, Chem. Eng. Sci. 57 (2002). 249–245.
[133] L. Gherardini, P.A. Michaud, M. Panizza, Ch. Comninellis, N. Vatistas, Electrochemical oxidation of 4-Chlorophenol for waste water treatment. Definition of normalized current efficiency, J. Electrochem. Soc. 148 (2001). D78–D84.47.
[134] J. Wu, F. Liu, H. Zhang, J. Zhang, L. Li, Decolorization of CI Reactive Black 8 by electrochemical process with/without ultrasonic irradiation, Desalin. Water Treat. 44 (2012) 36–43.

[135] W. Jiade, M. Yu, L. Chenliang, C. Jianmeng, Chlorobenzene degradation by electro-heterogeneous catalysis in aqueous solution: intermediates and reaction mechanism, J. Environ. Sci. 20 (2008) 1306–1311.
[136] C. Ratiu, F. Manea, C. Lazau, I. Grozescu, C. Radovan, J. Schoonman, Electrochemical oxidation of p-aminophenol from water with boron-doped diamond anodes and assisted photocatalytically by TiO_2-supported zeolite, Desalin. 260 (2010).
[137] M. Panizza, A. Kapalka, Ch. Comninellis, Oxidation of organic pollutants on BDD anodes using modulated current electrolysis, Electrochim. Acta 53 (2008) 2289–2295.
[138] Á. Anglada, A. Urtiaga, I. Ortiz, D. Mantzavinos, Evan Diamadopoulos, Boron-doped diamond anodic treatment of landfill leachate: Evaluation of operating variables and formation of oxidation by-products, Water Res. 45 (2011) 828–838.